(12) INTERNATIONAL APPLICATION PUBLISHED UNDER THE PATENT COOPERATION TREATY (PCT)

(19) World Intellectual Property Organization
International Bureau

(43) International Publication Date
03 October 2024 (03.10.2024)

WIPO | PCT

(10) International Publication Number
WO 2024/200545 A1

(51) International Patent Classification:
A61B 17/34 (2006.01) *A61B 5/06* (2006.01)
A61B 34/20 (2016.01)

(21) International Application Number:
PCT/EP2024/058305

(22) International Filing Date:
27 March 2024 (27.03.2024)

(25) Filing Language: English

(26) Publication Language: English

(30) Priority Data:
23165112.6 29 March 2023 (29.03.2023) EP
23203066.8 11 October 2023 (11.10.2023) EP

(71) Applicant: **SYDDANSK UNIVERSITET** [DK/DK]; Campusvej 55, 5230 Odense M (DK).

(72) Inventors: **CHENG, Zhuoqi**; c/o Syddansk Universitet, Campusvej 55, 5230 Odense M (DK). **ERIKSEN, René Lynge**; c/o Syddansk Universitet, Campusvej 55, 5230 Odense M (DK). **SAVARIMUTHU, Thiusius Rajeeth**; c/o Syddansk Universitet, Campusvej 55, 5230 Odense M (DK).

(74) Agent: **PLOUGMANN VINGTOFT A/S**; Strandvejen 70, 2900 Hellerup (DK).

(81) Designated States *(unless otherwise indicated, for every kind of national protection available)*: AE, AG, AL, AM, AO, AT, AU, AZ, BA, BB, BG, BH, BN, BR, BW, BY, BZ, CA, CH, CL, CN, CO, CR, CU, CV, CZ, DE, DJ, DK, DM, DO, DZ, EC, EE, EG, ES, FI, GB, GD, GE, GH, GM, GT, HN, HR, HU, ID, IL, IN, IQ, IR, IS, IT, JM, JO, JP, KE, KG, KH, KN, KP, KR, KW, KZ, LA, LC, LK, LR, LS, LU, LY, MA, MD, MG, MK, MN, MU, MW, MX, MY, MZ, NA, NG, NI, NO, NZ, OM, PA, PE, PG, PH, PL, PT, QA, RO, RS, RU, RW, SA, SC, SD, SE, SG, SK, SL, ST, SV, SY, TH, TJ, TM, TN, TR, TT, TZ, UA, UG, US, UZ, VC, VN, WS, ZA, ZM, ZW.

(54) Title: SPATIAL POSITIONING SURGICAL DEVICE

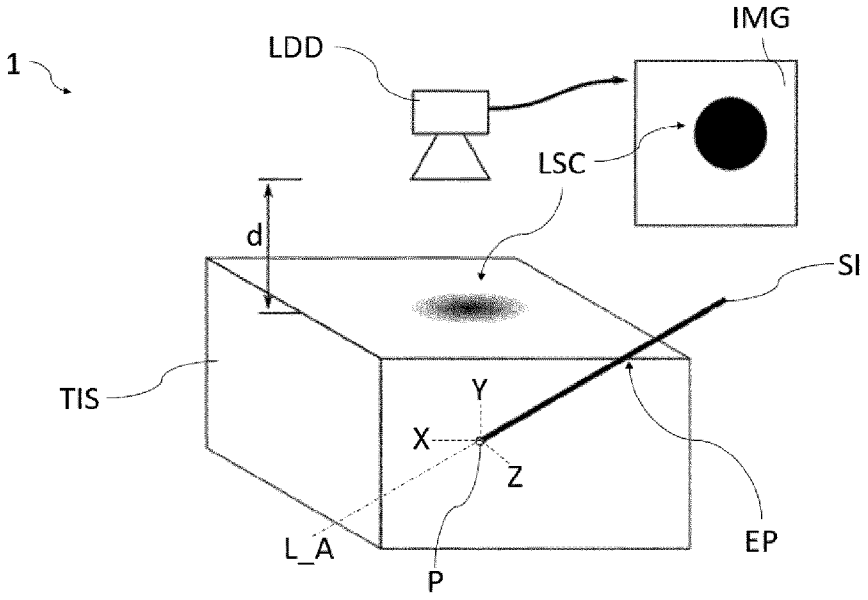

Fig. 3

(57) Abstract: The invention relates to a system and method for providing the depth and orientation of a surgical instrument inserted into biological tissue. The system comprises a surgical instrument adapted to emit light into the biological tissue and a light detection device outside said tissue, and wherein an algorithm is adapted to provide said depth and orientation information, based on light scatter detected by the light detection device; and a peripheral user interface adapted to receive and display said information to a user if the surgical instrument, such as a health care person. In particular, the invention is advantageous for deep vessel insertion or aiding e.g. a nurse in reaching a small blood vessel of e.g. an infant or small child with a cannula. Further, the invention is advantageous for training health care personnel to improve their needle insertion technique, such as with a training phantom and provide decision support during needle insertion.

WO 2024/200545 A1

[Continued on next page]

(84) Designated States *(unless otherwise indicated, for every kind of regional protection available)*: ARIPO (BW, CV, GH, GM, KE, LR, LS, MW, MZ, NA, RW, SC, SD, SL, ST, SZ, TZ, UG, ZM, ZW), Eurasian (AM, AZ, BY, KG, KZ, RU, TJ, TM), European (AL, AT, BE, BG, CH, CY, CZ, DE, DK, EE, ES, FI, FR, GB, GR, HR, HU, IE, IS, IT, LT, LU, LV, MC, ME, MK, MT, NL, NO, PL, PT, RO, RS, SE, SI, SK, SM, TR), OAPI (BF, BJ, CF, CG, CI, CM, GA, GN, GQ, GW, KM, ML, MR, NE, SN, TD, TG).

Declarations under Rule 4.17:

— *of inventorship (Rule 4.17(iv))*

Published:

— *with international search report (Art. 21(3))*

— *in black and white; the international application as filed contained color or greyscale and is available for download from PATENTSCOPE*

SPATIAL POSITIONING SURGICAL DEVICE

FIELD OF THE INVENTION

The present invention relates to a device, system and method adapted to detect and provide spatial orientation and position of a surgical instrument in tissue.

BACKGROUND OF THE INVENTION

The invention aims to address the challenge of e.g. needle tip tracking during a deep percutaneous insertion. Such operation is often requested in healthcare such as deep vein/artery intervention, deep brain stimulation (electrodes insertion) and biopsy. Conventionally, the location and orientation of the needle tip is estimated empirically by the operator, and thus, it is hard to guarantee hitting a targeted region especially in a deep tissue region. In addition, significant deflection of needle and tissue rupture occurs during the insertion, making the tracking task even more difficult.

Hence, an improved method and a system would be advantageous.

OBJECT OF THE INVENTION

It is a further object of the present invention to provide an alternative to the prior art.

In particular, it may be seen as an object of the present invention to provide a method and system that solves the above mentioned problems of the prior art with providing spatial information relating to percutaneous insertion of surgical instruments into tissue and further to provide information relating to adjacent tissue structures and a verification method related to the surgical instrument entering a specific target region of said tissue, such as verification that a blood vessel has been punctured.

SUMMARY OF THE INVENTION

Thus, the above-described object and several other objects are intended to be obtained in a first aspect of the invention by providing a computer implemented method of determining the spatial position and orientation of a surgical instrument, such as a cannula or catheter, when the surgical instrument is positioned within tissue of a subject, the computer implemented method comprising:

-emitting light from a portion of the surgical instrument at least when said portion is positioned within tissue,

-providing a light detection device outside of said tissue,

-detecting light scatter from within the tissue, with the light detection device,

-providing an algorithm adapted to determine the spatial position and orientation of the instrument relative to a reference point, based on the light scattered from within the tissue,

-providing the position and orientation of the surgical instrument to a user.

The invention is particularly, but not exclusively, advantageous for obtaining spatial information relating to the inserting of a surgical instrument, such as a cannula, percutaneously of a patient.

In an alternative embodiment, the present invention relates to a computer implemented method of determining the spatial position and orientation of a surgical instrument within tissue, the computer implemented method comprising:

-emitting light from a portion of the surgical instrument,

-providing a light detection device outside of said tissue,

-detecting light scatter from within the tissue, with the light detection device,

-providing an algorithm adapted to determine the spatial position and orientation of the instrument, relative to a reference point, into said tissue, based on the light scattered from within the tissue,

-providing the position and orientation of the surgical instrument to a user.

It is to be understood, that the computer implemented method according to the invention does not construe surgical steps, such as performing any control or movements to the surgical instrument, but provides spatial information as to the

position and orientation of said surgical instrument to a user; and furthermore may provide a signal when detecting a change of light scatter related to a change in tissue type at or near the surgical instrument.

In particular, the invention provides an advantageous method for providing a physician information, to faster, easier and with less inconvenience to a patient to insert e.g. a needle or cannula into a vein or an artery of a patient. Thus, in some embodiments, the surgical instrument is comprised of an outer cannular, and an inner needle, and wherein the inner needle is adapted with light emitting means. In these embodiments, when a desired target is reached, the inner needle is removed while the outer cannula is kept in place at said target, and a secondary surgical device can be positioned within said outer cannula.

In yet other embodiments, the surgical instrument is comprised of a first and at least a second lumen, and wherein one lumen is suitable for emitting light and the at least second lumen is suitable for e.g. the insertion of a peripheral device, such as a cannula, needle or other relevant device.

The invention is further advantageous for providing a method of aiding a physician in reaching e.g. a certain part of percutaneous tissue for e.g. tissue biopsy extraction or e.g. deep vessel insertion. It should be noted that the present invention is not limited to entry points of the skin of a patient, but would also be advantageous for guiding a surgical instrument into tissue through e.g. the oral, nasal cavity, vaginal cavity or rectal cavity, wherein the surgical instrument penetrates the tissue from e.g. the oral cavity.

It is to be understood, that guiding is to be construed as continuously providing spatial information relating to the surgical instrument, to the user.

In yet other embodiments, the invention may be advantageous for aiding dentists, ophthalmologist and veterinarians, where surgical instruments may be inserted into tissue of a patient.

Even further, the invention may be advantageous for aiding a physician or nurse in reaching a vein of very young patients, such as an infant or small child, to reduce pain or discomfort to said young patient.

In the context of the present invention, spatial position and orientation is to be understood, as the use of information provided to a user relating to the part of the surgical instrument which is not in view of the user due to said instrument being inserted into and beyond a tissue surface, such as the skin of a patient.

It is further to be understood that the surgical instrument may comprise one or more lumens and wherein, in some embodiments, at least one of said lumens can be used for e.g. technical features of the invention, such as for containing a light source, optical fibre, processing means or other relevant parts of the invention as disclosed; and wherein at least one other of said one or more lumens may be used for e.g. extraction of or injection of a substance. In some embodiments, a lumen of the instrument may be suitable for the injection or extraction of a fluid. In other embodiments, a lumen of the instrument may be suitable for the insertion or extraction of a solid or semi-solid member, such as for extraction of a biopsy or insertion of an implant. In yet other embodiments, a lumen of the instrument may be used as a catheter for insertion into a tissue or a lumen of the patient.

In a preferred embodiment, the light emission is directed from a tip end of the surgical instrument, such as in a conical or fan-like direction from said tip end, towards tissue substantially in front of an insertion direction of said tip end. In other embodiments, the light is emitted e.g. 90°, 180° or 360° around a periphery of the surgical instrument. In yet other embodiments, a plurality of light emitting devices is adapted to the instrument, to enable the detection of light both around a periphery of and directly in front of said instrument. It is to be understood that light emitted from each of the plurality of light emission sources may be distinct or similar.

In an example, some of the light emitted, is emitted at a first wavelength or with a temporal pattern and/or spatial pattern, and light emitted from e.g. second

and/or third sources may be transmitted or provided at different wavelengths or with differing temporal patterns or spatial patterns.

In an advantageous embodiment of the invention, the spatial pattern provided from one or more light sources may be a tailored output phase profile adapted to create astigmatic light beams. This embodiment is particularly advantageous for detecting the light scatter within tissue.

In another advantageous embodiment, the spatial pattern provided from one or more light sources may be higher order guided modes. In some embodiments, the light provided at the surgical instrument is a lens, in other embodiments, the light is provided from an optic fiber.

In yet another advantageous embodiment, the spatial pattern provided from one or more light sources may be higher order guided modes from an optical fiber such as doughnut beams.

In yet another advantageous embodiment, the spatial pattern provided from one or more light sources may be non-diffracting Bessel beams.

The above embodiments may be combined, and provides the advantage of enabling better detection of the position, orientation and puncture detection of the surgical instrument, based on light scattered, wherein the one or more lights sources is adapted with a spatial pattern.

Thus, from the above, it is to be understood, that the surgical instrument may be adapted with a plurality of light sources, and wherein one or more may be adapted with a lens and one or more may be adapted with a temporal pattern.

The above embodiments are particularly advantageous , as using at least two, or a plurality of light beams with different focus points in the tissue, can be discriminated by modulating each beam with a distinct modulation frequency, thus the origin of the beam is known by proper demodulation.

In some embodiments, the light emitted may be a combination of one or more white light, spectrums of light, polarized light, coherent light, temporally patterned light and/or lights emitted at different wavelengths.

In the context of the present invention, light detection is to be understood as a means of detecting light, such as a photo-sensor, photodiode(s), Complementary metal–oxide–semiconductor (CMOS), charge-coupled devices (CCD's) or a camera, photo-voltaic sensor (array) or other suitable device.

In the context of the present invention, light scatter is to be understood as the physical phenomenon that occurs when light interacts with turbid materials or particles in biological tissues, causing it to be absorbed, depolarized, change direction and scatter in multiple directions. The present invention is adapted to utilize said light scatter, when detected, to define the spatial position and orientation of the surgical instrument, based on algorithms or mathematical models adapted to calculate the spatial information based on said detected light and/or light scatter.

In the context of the present invention, entry point is to be understood as the point at which the surgical instrument is entering the tissue of the subject, through the skin, i.e. an analogue spatial reference which is visible to the physician during the procedure.

In the context of the present invention, spatial information relates to e.g. a longitudinal axis of the surgical instrument, in an x-y-z plane within said tissue, and the position of a tip-end or other relevant spatial information relevant to a user during a procedure.

In the context of the present invention, reference point is to be understood as a defined and static spatial coordinate relative to the point at which light is emitted from the surgical instrument. In some embodiments, the reference point is the light detection device.

In a preferred embodiment of the invention the algorithm is a machine learning algorithm, the method further comprising:

-providing said machine learning algorithm with a training set adapted to train the machine learning algorithm to determining the position and orientation of the surgical instrument emitting light within a tissue, the training set being based on predetermined spatial positions, orientations and light scatter patterns of light emitted from tissue.

This embodiment is particularly advantageous for providing a method, wherein the algorithm is enabled to be trained on verified training sets, ensuring a more precise determination of spatial position of the surgical instrument.

The learning algorithm may be selected from one or more of a convolutional neural network or fundamental image processing in combination with multi-layer perceptron (MLP).

In other embodiments, the algorithm may be another type of Artificial Intelligence algorithm.

Artificial Intelligence (AI) refers to the theory and development of computer systems capable of performing tasks that historically required human intelligence. These tasks include recognizing speech, making decisions, and identifying patterns. AI is an umbrella term that encompasses a wide variety of technologies.

One such technology under AI is Machine Learning, which uses algorithms trained on data sets to create models that enable machines, such as the present invention, to perform tasks without explicit instructions. In particular, these tasks include categorizing images and analyzing data.

A specific type of machine learning model is a Neural Network. These models make decisions in a manner similar to the human brain, using processes that mimic the way biological neurons work together to identify phenomena, weigh options, and arrive at conclusions. Every neural network consists of layers of nodes, or artificial neurons—an input layer, one or more hidden layers, and an output layer. Each node connects to others, and has its own associated weight and threshold.

A specialized type of neural network is a Convolutional Neural Network (CNN). CNNs excel in processing structured grid data, such as images. They are composed of one or more convolutional layers, often followed by pooling layers, then one or more fully connected layers. With respect to the present invention, the convolutional layer uses a set of learnable filters, which are small spatially but extend through the full depth of the input volume. Their application to the input results in activation maps that give the responses of that filter at different spatial positions. CNNs are specifically designed for tasks like image recognition, which makes them a specialized tool within the machine learning toolkit, and particularly advantageous within the present invention.

In a preferred embodiment of the invention, the method further comprises detecting a first tissue based on the light scatter and detecting a second tissue based on a change in the light scatter; providing the user with information that a second tissue has been detected. This embodiment is particularly advantageous for providing the user with information related to whether the tissue structure has changed, thus providing a verification that e.g. a venous tissue has been reached by the user. Thus, the embodiment may be able to verify e.g. a puncture of a vein or artery performed by the user, based on a change in light scatter.

In another preferred embodiment of the invention, the method further comprises:
-providing light scatter information relating to tissue structures, such as blood vessels, nerves or bone, adjacent to the light emitted from the surgical instrument and providing the user with spatial tissue structure information relative to a current position of the surgical instrument.

In the context of the present invention, tissue structure information is to be understood as the change in scatter pattern and absorption of light between different densities and other properties of different tissues, which in turn can be utilized by the invention to provide further information to the user. As an example, the invention is enabled to distinguish between muscle and a tumor based on detected light scatter and provide said information to the user.

In yet another preferred embodiment of the invention, the method further comprises:

-providing verification to the user relating to the surgical instrument entering a tissue structure, such as a blood vessel, within the tissue, based on the detected light scatter from within said tissue structure.

It is to be understood, that the computer implemented method does not involve the surgical step of moving the surgical instrument within tissue, but to convey spatial information relating to the surgical instrument to a user.

This embodiment is particularly advantageous for providing a verification of e.g. a tip of the surgical instrument having reached a target, such as a blood vessel. It is to be understood that the target may be any relevant physiological target, such as a tumor, blood vessel, a specific region or other.

It is to be understood that as the surgical instrument, such as a needle tip, punctures and enters specific tissues such as blood vessels, a high amount of emitted light at specific wavelengths is suddenly absorbed by the tissue, causing a sudden change of scattering pattern detected by the light detection device. The absorption rates of different tissues are different. When a light source of 900 nm is used, the absorption coefficients of HbO2, Hb, skin, subcutaneous tissues and muscles are 6, 5, 0.8, 1.07 and 0.32 respectively (unit: cm^{-1}). This indicates a significant decrease of intensity of the scattering image which can be detected when the needle tip punctures the blood vessel, thus enabling for verification to a user reaching a specific target such as said blood vessel.

In an advantageous embodiment of the invention, the method further comprises mapping tissue structures adjacent to the instrument, based on the light scatter and providing a spatial overview of the tissue to the user.

In the context of the present invention, adjacent is to be understood as e.g. mapping tissue between 1 and 10 cm from the point at which light is emitted from the surgical instrument. Further, in some embodiments, the invention is enabled to map further in one spatial direction than in another spatial direction. In a preferred embodiment, the mapping can be performed distally from a longitudinal axis of the surgical instrument from between 0.1 to 20 cm from a tip end of the surgical instrument.

In a preferred embodiment of the invention, the method further comprises:

-receiving an input from the user relating to a selected target within the tissue,

-guiding the user to translate the surgical device to said target based on detected light scatter,

and when the surgical instrument is positioned at or within said target,

-verifying the position of the surgical instrument at or within said target to the user.

It is to be understood, that the computer implemented method does not involve the surgical step of moving the surgical instrument within tissue, but to convey spatial information relating to the surgical instrument to a user.

In another preferred embodiment of the invention, the method further comprises:

-receiving an input from the user relating to a selected target within the tissue,

-providing a current position and orientation of the surgical instrument to the user;

and when the surgical instrument is positioned at or within said target,

-verifying the position of the surgical instrument at or within said target to the user.

It is to be understood, that the computer implemented method does not involve surgical steps, such as moving a surgical instrument, but to continuously provide spatial information relating to the surgical instrument, to a user, such as a medical professional.

This embodiment is particularly advantageous for aiding a physician in e.g. reaching a blood vessel fast, reducing the discomfort applied to a patient during the procedure.

The above is known as verification or detection of puncture.

Two methods can be used for the puncture detection.

The first method is based on single image input and the second method is based on image sequences.

For the first method, a neural network such as convolutional Neural Network (CNN) or ResNet is used and trained, to identify a puncture event directly based on the acquired image.

The second method uses a time sequence of images or a video clip as input for the Neural Network in order to determine whether the surgical instrument tip enters a different material, i.e. tissue. To achieve this goal, the Network architecture may be a CNN+LSTM or 3D CNN.

In an embodiment of the invention, the method further comprises applying a graphics processing units (GPU's) to train and perform the machine learning algorithm.

The GPUs may be used for training and performing the machine learning algorithm. The parallel processing capabilities of GPUs accelerate the training of neural networks. Further, the processing time can be reduced to sub-millisecond when the algorithm is performed on a computer comprising graphical processing units (GPUs). This observation suggests that the proposed system is sufficiently fast for real-time tracking of the needle tip, even when implemented on a portable setup.

In a second aspect, the invention relates to a spatial positioning and orientation system for a surgical instrument, the system comprising:

-a light detection device arranged outside the tissue,

-a user interface in data communication with the light detection device,

-an instrument adapted to emit light from a portion of said instrument within tissue, when said portion of the instrument is positioned within tissue,

-a processor adapted to execute an algorithm, said algorithm determining a spatial position and orientation of the surgical instrument within the tissue, based on light scattered from within the tissue and detected by the light detection device, wherein the system is configured to provide the spatial position and orientation of the surgical instrument to a user through the user interface, while said user operates the surgical instrument within tissue of a subject.

In a preferred embodiment of the invention, the light detection device is a camera positioned at least above an entry point of the tissue, the entry point being the point of entry of the surgical device into the tissue of the subject, the system further comprising a distance measuring device adapted to measure a distance between the entry point and said camera, the device adapted to calibrate the measured light scatter from the tissue to the camera. It is to be understood that at least above is to be understood as e.g. between 5 to 100 cm from said entry point.

In another preferred embodiment of the invention the light detection device is a sensory array, preferably a patch with an array of sensors, adapted to be adhered to skin of a subject, near an entry point, into tissue of said subject, the sensory array comprising photo-sensors adapted to detect light scatter from within said tissue. It is to be understood that near is to be understood as e.g. between 1 to 50 cm from the entry point, depending on where the surgical instrument is to be inserted into the tissue. This embodiment is particularly advantageous, as the use of a photo sensitive / photo detector patch/array compared to a traditional photon counting sensor (CCD or CMOS) allows faster sampling rates kHz-MHz, thus amplitude modulation of the light signal is possible, allowing for lock-in amplification, improving signal to noise ratio.
In yet another preferred embodiment of the invention, the surgical instrument comprises one or more light sources, such as an LED or an array or LED's, the light source(s) positioned at or near a distal tip of the surgical instrument.

In an advantageous embodiment of the invention, the surgical instrument is adapted with a lumen comprising one or more optical fibres adapted to emit light at or near a distal tip of the surgical instrument.

In some embodiments, the surgical instrument comprises a second lumen adapted for physiological purpose, such as for injecting or extracting matter to/from the patient.

In a preferred embodiment of the invention, the system comprises a plurality of light sources which is adapted to emit light at different wavelengths and/or or at different temporal intervals, to generate a specific pattern of light emitted.

In some embodiments, the light sources are adapted e.g. at a tip-end of the surgical instrument.

In yet other embodiments, the light sources are provided at various locations along a length and periphery of the surgical instrument.

It is further to be understood that at least some of said light sources are positioned at length of said surgical instrument, which is within the patient's tissue during normal operation of the surgical instrument.

In another preferred embodiment of the invention, the system is a decision support system and wherein the system is adapted to guide the user to reach a target of the tissue with the surgical instrument, said target being specified by said user through the user interface.

In yet another preferred embodiment of the invention, the user interface comprises visible or audible output adapted to guide the user to operate the surgical instrument within tissue.

This embodiment may be particularly advantageous for teaching purposes, wherein decision support provided through auditory or visual stimulus may increase the proficiency of a user, in turn reducing distress and discomfort to patients.

In yet another advantageous embodiment of the invention, the surgical instrument is adapted as a bioimpedance sensor, to provide further information relating to tissue of the subject.

Electrical bioimpedance (EBI) method has been demonstrated with high sensitivity in venipuncture detection. The electrical bioimpedance can be measured based on one electrode configuration or multiple electrodes configurations. An external ground electrode may also be required to be attached to the body. The measured impedance value can indicate the likelihood of blood contact at the needle tip, since blood is more conductive compared to skin and fat.

The venipuncture can be detected through combining two sensing modalities, the proposed optical method and EBI. The sensor fusion methods can be one of the following, but not limited to, Bayesian fusion, covariance intersection, fuzzy logic or decision tree.

In an embodiment of the invention, if the surgical instrument is expected to be placed in an artery or a vein, then an electrical bioimpedance measurement verify that the instrument is placed in an artery or a vein.

If the instrument is expected to be placed in an artery or a vein due to the method of determining a spatial position and orientation of the surgical instrument, then by measuring the electrical bioimpedance, it can be verified that the instrument indeed is placed in an artery or a vein as the electrical bioimpedance can determine the kind of tissue the instrument is in.
Thus, it is to be understood, that the combination of multiple sensor modalities, such as optical and bioimpedance sensors, can be used by the algorithms to detect both a spatial position and orientation of the surgical instrument as well as verifying whether the surgical instrument is positioned within an artery or vein; or other tissue where electrical conductivity can be used to determine tissue type.

In a preferred embodiment of the invention, the user interface is a peripheral device, such as a tablet or a computer wherein the peripheral device is adapted to receive data wirelessly from the spatial positioning and orientation system.

In another preferred embodiment of the invention, the surgical instrument is adapted with a lens, said lens adapted to focus the light emitted from the surgical instrument.

In yet another preferred embodiment, the surgical instrument is adapted with a collimator, said collimator adapted to collimate the light emitted from the surgical instrument. In some embodiments, the surgical instrument is adapted with a lens and a collimator, to provide a specific light beam profile.

In an embodiment the processor applies graphics processing units (GPU's) to train and perform a machine learning algorithm.

The processing time can be reduced to sub-millisecond when the algorithm is performed on a computer comprising graphical processing units (GPUs), suggesting that the method is sufficiently fast for real-time tracking of the needle tip, even when implemented on a portable setup.

In a preferred embodiment the sensory array comprises at least 8x8 sensors, preferably at least 16x16 sensors, even more preferred at least 32x32 sensors.

In another preferred embodiment, the sensory array comprises between 32x32 and 128x128 sensors.

In yet other embodiments, the sensory array comprises between 16x16 and 512x512 sensors or such as between 32x32 and 256x256 sensors.

In a third aspect, the invention relates to a surgical instrument, preferably a cannula, comprising:

-a light source at or near a distal tip of the instrument,
-a light detection device at a proximal location of the instrument,
-a processor adapted to receive and process a signal received from the light detection device,
-a wireless transmitter adapted to transmit processed data from the processor to an associated peripheral device, such as a computer, and
-optionally an energy storage device, such as a battery,
wherein the surgical instrument is configured to detect light scatter from within tissue, when at least the distal tip of the surgical device is inserted into said tissue and provide information relating to tissue structures adjacent to the light source, to a user through said associated peripheral device.

This aspect of the invention is particularly, but not exclusively, advantageous in that the surgical instrument may comprise all the technical features in a single, hand-held instrument.

In a preferred embodiment of the invention, the surgical instrument is substantially sealed, enabling for easy sanitation between use.

In a fourth aspect, the invention relates to use of a system or device according to the second or third aspect of the invention for injecting a substance or obtaining a biological sample from a patient.

In a fifth aspect, the invention relates to a method of training an algorithm to determine the spatial position and orientation of the surgical instrument according to the system of the second aspect or the surgical instrument of the third aspect of the invention, the training method comprising:
-providing the algorithm with a training set adapted to train the algorithm to determine the position and orientation of the surgical instrument emitting light within a tissue, the training set being based on predetermined spatial positions, orientations and light scatter patterns of light emitted from tissue.

In a preferred embodiment, the training set comprises at least a first set of images obtained from outside of the tissue, and a data set comprising a measured position and orientation of the surgical instrument within the tissue.

In another preferred embodiment, algorithm is further trained to detect the transition of position of the surgical instrument, from a first tissue to a second tissue.

In yet another preferred embodiment, the training set further comprises images obtained from outside of the tissue, wherein the surgical instrument emits light within the first tissue, and images wherein the surgical instrument emits light within the second tissue, training the algorithm to detect a change in tissue.

In an advantageous embodiment, the algorithm is selected from one or more of a convolutional neural network or fundamental image processing in combination with multi-layer perceptron.

The first, second, third, fourth and fifth aspect of the present invention may each be combined with any of the other aspects. These and other aspects of the invention will be apparent from and elucidated with reference to the embodiments described hereinafter.

BRIEF DESCRIPTION OF THE FIGURES

The method and system according to the invention will now be described in more detail with regard to the accompanying figures. The figures show one way of implementing the present invention and is not to be construed as being limiting to other possible embodiments falling within the scope of the attached claim set.

Fig. 1 shows an illustration of the system and method according to an embodiment of the invention.

Fig. 2 shows an illustration of the system and method according to another embodiment of the invention.

Fig. 3 shows another illustration of the system and method according to an embodiment of the invention.

Fig. 4 shows an illustration of the surgical instrument, according to an embodiment of the invention.

Fig. 5 shows an illustration of the system and method according to yet another embodiment of the invention.

Fig. 6 shows another illustration of the system and method according to yet another embodiment of the invention.

Fig. 7A and Fig. 7B show a chart of a proof-of-concept simulation study.

Fig. 8A to 8E show the scattering pattern detected by a light detection device, from a tissue surface.

Fig. 9 shows an illustration of the surgical instrument SI, according to another embodiment of the invention.

Fig. 10 shows a flow-chart of a method according to an embodiment of the invention.

Fig. 11 shows a simplified model that treats the skin and adipose tissues together as a homogeneous material.

Fig. 12 shows a visual representation of the model architecture.

Fig. 13 shows L2 norm errors in different insertion depths Z*.

Fig. 14 shows that the error in the near-surface area is not higher than that in the subsurface region.

Fig. 15 shows examples of imaging from two different depths for both the bacon and fresh pork phantoms.

Fig. 16 shows a graph, the graph representing a performance study perform in relation to different image resolutions.

Fig. 17 shows a confusion matrix, related to a study of puncture detection accuracy by use of the algorithm according to an embodiment of the invention.

DETAILED DESCRIPTION OF AN EMBODIMENT

Fig. 1 shows an illustration of the system 1 and method according to an embodiment of the invention. Fig. 1 shows an arm of a subject SUB, with a surgical instrument SI inserted into tissue of the subject SUB. The surgical instrument SI is adapted with light emission means at a tip end, providing a light from within the tissue of the subject SUB, the light illustrated by light scatter LSC detected by the light detection device LDD. In particular, in Fig. 1, the light detection device LDD is depicted as a camera, but may be another suitable photo sensor adapted to detect light scatter LS. In this embodiment, the distance d, between the light detection device LDD and the entry point EP of the surgical instrument SI is known, either by measuring the distance manually or by providing a distance measurement device (not shown) enabled to provide the distance to the system 1. In other embodiments, the distance d1 is measured perpendicular from the surface of the tissue to the light detection device or a distance measurement device.

Fig. 2 shows an illustration of the system 1 and method according to another embodiment of the invention. Fig. 2 shows an arm of a subject SUB, with a surgical instrument SI inserted into tissue of the subject SUB. The surgical instrument SI is in optical connection to a light source LS, to provide a light from within the tissue of the subject SUB, the light illustrated by light scatter LSC detected by the light detection device LDD. In particular, in Fig. 2, the light detection device LDD is depicted as a camera, but may be another suitable photo sensor adapted to detect light scatter LS. In this embodiment, the distance d, between the light detection device LDD and the entry point EP of the surgical

instrument SI is known, either by measuring the distance manually or by providing a distance measurement device (not shown) enabled to provide the distance to the system 1. In other embodiments, the distance d1 is measured perpendicular from the surface of the tissue to the light detection device or a distance measurement device.

Fig. 3 shows another illustration of the system 1 and method according to an embodiment of the invention. Fig. 3 shows tissue TIS represented by a 3D segment, with a surgical instrument SI inserted into the tissue TIS. The horizontal upper surface of the tissue TIS represents an outer layer of tissue, from which the light detection device LDD can measure light scatter LSC. The surgical instrument SI is adapted to emit light from within the tissue TIS, the light illustrated by light scatter LSC detected by the light detection device LDD. In this embodiment, the distance d, between the light detection device LDD and the entry point EP of the surgical instrument SI is known, either by measuring the distance manually or by providing a distance measurement device (not shown) enabled to provide the distance to the system 1. The light detection device LDD obtains an image IMG of the light scatter, in which an algorithm of the system 1 is adapted to convert the detected light scatter LSC into X, Y and Z coordinates of the tip end P of the surgical instrument SI within the tissue, relative to the entry point EP; and the spatial orientation of the longitudinal axis L_A of the surgical instrument SI. In other embodiments, the distance d1 is measured perpendicular from the surface of the tissue to the light detection device or a distance measurement device.

Fig. 4 shows an illustration of the surgical instrument SI, according to an embodiment of the invention. Fig. 4 shows the tip end TE of the surgical instrument SI, the surgical instrument comprising a plurality of lumens LU within the outer periphery OP of the surgical instrument SI. It is to be understood that one or more of the plurality of lumens LU may contain at least one light source or a plurality of light sources and/or optic fibres, the optic fibres adapted to emit light from a light source (not shown) in optic connection with said optical fibres.

Further, the light source at the needle tip may be programmable by light transferred through a multi-core optic fiber. Through controlling the

on/off/intensity of the lighting of each core, the scattering pattern can be different and used for further tracking/detection purposes.

Even further, the proposed invention may be combined with other sensing methods via sensor fusion for a detection task. For instance, the needle tube itself can be used as an electrode for electrical bioimpedance sensing. The measured bioimpedance signal can be fused with the optical method in a tissue detection task.

Fig. 5 shows an illustration of the system 1 and method according to yet another embodiment of the invention. Fig. 5 shows a light detection device LDD, positioned on the skin of a subject SUB. In this particular embodiment, the light detection device LDD is a patch adhered to the skin, the patch comprising an array or matrix of photo sensors as shown by the white rectangles of the light detection device LDD. The light detection device LDD is adapted to detect light scatter from within tissue of the subject SUB, and wherein the light is emitted from a light source LS in optical connection with the surgical instrument SI.

Further, the embodiment according to Fig. 5 may be used for generating a closed-loop control in a robotic system. Such robotic system can achieve automatic needle insertion to a pre-defined spatial location, based on spatial information provided by the system and method.

It is to be understood that the level of melanin of epidermis may affect the accuracy of the proposed method. This obstacle may be solved by e.g. capturing the skin colour of the specific subject, at the beginning of the procedure and input this value to the algorithm.

Fig. 6 shows another illustration of the system 1 and method according to yet another embodiment of the invention. Fig. 5 shows the surgical instrument SI being inserted into a blood vessel BV within tissue TIS. The surgical instrument SI is optically connected to a first and second light source LS, LS*, each of the light sources LS, LS* emitting light at different wavelengths WL, WL*, such as at 680 nm and 850 nm respectively. The first and second light sources LS, LS* is operated by a switch SW. The first and second light sources LS, LS* is connected

to the surgical instrument SI through an optical combiner, so as to enable for both light sources LS, LS* to emit light through a single optical fibre (not shown) of the surgical instrument SI. In other embodiment, each of the first and second light source LS, LS* may be individually connected to respective optical fibres of the surgical instrument. In yet other embodiments, a single light source may be adapted to emit light at different wavelengths. Light scattered from the blood vessel and tissue is detected by the light detection device LDD, generating first and second images IMG, IMG*, showing a more intense light scatter in the first image IMG, relative to the light scatter of the second image IMG*, as light scatter using a first wavelength WL, such as 680 nm scatters more in blood, than when using a second wavelength WL*, such as 850 nm.

Further, the proposed invention can be used for tissue identification through applying a lighting spectrum. An example is shown in Fig. 6, in which a switch SW controls two lighting sources LS, LS* of 660 nm and 850 nm respectively, to generate the scatter image. Since the absorption rates of different tissues are different, the generated scatter images by two sources can be compared. Specifically, the differential of scatter image between two sources can be used as input of a machine learning algorithm. As an example, HbR absorbs more light of 660 nm than HbO2, while their absorption rates are similar for light sources of 850 nm. Therefore, if little change of the scatter image in terms of intensity and size is found between two lighting sources, the needle may be determined to have punctured into a vein. If the scatter image is bigger with a 660nm source compared to that with an 850nm source, it is more likely to have punctured an artery.

Fig. 7A and Fig. 7B show a chart according to a proof-of-concept simulation study. According to Fig. 7 A and Fig. 7B, the invention can be used for indicating the excitation of non-homogeneous anatomic features near the emitted light, such as emitted from a needle bevel NB. A simulation study is conducted as a proof of concept. Finite Element methods are used to simulate the scatting pattern. The left subfigures of Fig. 7A and Fig. 7B are the setup and physical elements of the study, showing depth from a tissue surface TS in mm in both x and y spatial direction where y is depth; and the right subfigures of Fig. 7A and Fig. 7B are the radiation intensity on the surface, as measured from the light detection device.

The simulation is simplified as a 2D model and light is emitted from the needle bevel NB.

According to the simulation results, when there is a non-homogeneous structure, such as a blood vessel BV as shown in Fig. 7B, above the needle bevel NB, it would cause the scattering pattern, i.e. intensity distribution to change, as seen on the line graph on the right side of Fig. 7B.

Fig. 8A to 8E show the scattering pattern detected by the light detection device, from a tissue surface TS, of, shape and intensity distribution, as it varies through 8A to 8E, from a change in depth and orientation of a beveled needle tip inside a phantom, the needle tip emitting light. The scatter image in different locations and angles: (A) z=15mm, θ=0, φ=45; (B) z=10mm, θ=0, φ=45; (C) z=15mm, θ=0, φ=60; (D) z=10mm, θ=90, φ=45; (E) z=10mm, θ=-90, φ=45.

It is to be understood that at least two methods can be implemented for estimating the needle tip position given the scattering image. Nevertheless, many other machine learning approaches such as Bayesian Neural Network or Fuzzy network may be applicable.

Method 1: fundamental image processing + multi-layer perceptron (MLP)
The illumination from the needle tip generates a scattering image on the tissue surface, which is captured by an external imaging sensor. The image is firstly processed through threshholding or multiple threshholding and provides a series of binary images. From the binary images, information of the black circle can be retrieved including centre position (x,y), size S, moment Mx and My. Then, a dataset can be generated with [x, y, S, Mx, My] as input; and the needle tip spatial position [X, Y, Z, Ox, Oy, Oz] as output is generated. It is to be understood that the output is a vector after normalization, and a Sigmoid function is used as the activation function of the output layer. An MLP neural network can be trained for the above regression.

Method 2: Convolution neural network (CNN)
CNN is generally capable of extracting image features owing to the integrated convolution layer. The input is the grey scale image from the imaging sensor and

the output is the tip spatial position. The basic CNN architecture passes the input grey scale image to a convolution layer and a pooling layer for feature extraction. The outputs from the pooling layer link to a fully connected network for determining the final output.

Fig. 9 shows an illustration of the surgical instrument SI, according to another embodiment of the invention. Fig. 9A shows a trimetric view of the tip end TE of the surgical instrument SI. Fig. 9B shows a cross section of the surgical instrument SI comprising two lumens, wherein the first lumen LU1 is adapted for surgical operations, such as for injecting or extracting a fluid. The second lumen LU2 is adapted with a light emission device LED, in this embodiment an optic fibre. Fig. 9C shows a cross section of the surgical instrument SI comprising two lumens, wherein the first lumen LU1 is adapted for surgical operations, such as for injecting or extracting a fluid. The second lumen LU2 is adapted with a light emission device LED, in this embodiment an optic fibre, and wherein a lens has been adapted within the second lumen to focus the light emitted from the optic fibre.

Fig. 10 is a flow-chart of a method according to an embodiment of the invention, the method comprising the following steps:
S1-providing a computer system in data communication with a light detection device, and when a surgical instrument adapted with a light emission device or light emission means is positioned within tissue:
S2-emitting light from a portion of the surgical instrument at least when said portion is positioned within tissue,
S3-providing the light detection device outside of said tissue,
S4-detecting light scatter from within the tissue, with the light detection device,
S5-providing an algorithm on said computer system adapted to determine the spatial position and orientation of the instrument, relative to a reference point or reference coordinate, into said tissue, based on the light scattered from within the tissue,
S6-providing the position and orientation of the surgical instrument to a user.

Deep needle insertion is a medical procedure that allows medical professionals inserting a needle from the skin and reach targets located beneath the surface,

such as tumors, nerves, or blood vessels. It plays a crucial role in enabling precise and targeted medical interventions such as administering medication, obtaining samples, or carrying out therapeutic procedures. Therefore, deep needle insertion is widely utilized across a diverse range of medical disciplines, including deep vessel interventions, biopsies, brachytherapy, interventional radiology, anaesthesia, and pain management.

Despite its wide applications, deep needle insertion presents inherent challenges and requires both expertise and technological support. One of the main difficulties encountered in this procedure is the deformation of soft tis-sue during insertion. As the needle penetrates the body, the surrounding tissues tend to move, making it challenging to precisely reach the intended target. Moreover, once the needle tip is within the tissue, its visibility becomes obscured, complicating the accurate tracking of its exact location. This lack of visibility becomes particularly problematic when encountering resistant tissues, as it frequently results in needle deflection, further impeding the ability to precisely locate the needle.

Frequently, healthcare professionals rely on imaging techniques to guide needle insertion, with ultrasound (US) and fluoroscopy being commonly used modalities. These imaging technologies provide real-time visualization of the needle and surrounding anatomical structures, aiding in the precise localization of the target, and facilitating adjustments to the insertion direction. However, the effectiveness of using this technique heavily depends on the practitioner's experience and necessitates extensive training to ensure proficiency. Advancements in robotics for needle deep insertion have been explored in the literature. A typical exploitation of robotic and artificial intelligence (AI) technology is through the extraction and detection of the needle tip from US images. Nevertheless, given the inherent noise in US imaging, the utilization of complex image processing algorithms and substantial computing power is required.

In addition to the previously described image-guided needle insertion method, needle guidance technology can also incorporate embedded sensors, particularly for the task of needle tip tracking (NTT). Previous studies have explored the use of concentric electrode needle for electrical bioimpedance sensing. But the

functionality of this technology is to detect the type of tissue in contact with the needle, rather than to provide the spatial position of the needle tip.

Alternatively, other studies have utilized electromagnetic (EM) sensors embedded in needle tips to enable tracking within a generated magnetic field. Research indicates that in favourable environments, an average accuracy of 1 mm can be achieved. However, the use of EM sensors presents several challenges. Firstly, calibration is required for seamless integration into the workflow. Secondly, the tracking accuracy is contingent on the absence of metal and magnetic fields in the environment. Lastly, the implementation of EM sensors can be relatively costly.

Alternatively, the NTT can be achieved by leveraging the accurate model of the needle deflection. Shape sensing techniques, such as strain gauges and Fiber Bragg Gratings (FBG), can be attached along the needle shaft to retrieve information on the needle's deflection. However, the FBG technology, while offering accurate needle shape reconstruction in real-time, is sensitive to temperature variations and can be relatively expensive to implement.
The objective is to present a novel sensing method for tracking the position of a needle tip accurately and in real time. The proposed method incorporates an optical fiber within the lumen of the needle to emit light at the needle tip. By capturing the light scattering imaging on the tissue surface, an AI-empowered image processing algorithm is employed to analyse the images and estimates the spatial position of the needle tip. The primary focus of this research is to utilize this technique for guiding needle insertion into deep vessels in the groin region, with the ultimate aim of enhancing patient care through improved effectiveness and efficiency. To the best of the authors' knowledge, the proposed NTT approach presents a pioneering advancement, and holds significant potential for extension to various other applications such as vessel puncture detection.

It is to be understood, that guiding is to be construed as providing spatial information to a user in relation to the surgical instrument.

The invention may be rephrased to a method for aiding surgical tools, such as needles, insertion to a non-homogeneous tissue area inside the body or organ.

The target tissue area may be in an irregular shape (tumor), but also can be in a tubular structure (vessels).

Despite training, achieving precise needle insertion to target a tumor situated deep within the body remains a challenge. Nevertheless, this procedure is frequently required for biopsy or treatment purposes. Typically, cancer treatments may require interventions with radioactive seed placement, Photodynamic Therapy (PDT) and target drug delivery.

It may also be interesting to introduce light to area near the tumor for PDT. PDT is a treatment that uses special drugs, sometimes called photosensitizing agents, along with light to kill cancer cells. The drugs only work after they have been activated by certain kinds of light. However, light cannot travel very far through body tissues. This limits its application to treating large cancers or cancers that have grown deeply into the skin or other organs. The invention can be applied for introducing optic needle to the target area and providing lighting during this treatment procedure.

During needle insertion, the needle bevel face can point downwards, or specifically, towards the vessel, instead of facing upwards. With this trick, the imaging is able to indicate the proximity of vessel, as well as increase the sensitivity of puncture detection. This is because more light can be absorbed by the blood right after the venipuncture with this trick.

As described, one of the primary applications for the proposed technology is to facilitate the guidance of needle insertion into the femoral artery in the groin area. The artery is ensconced within layers of adipose tissue and connective tissue beneath the skin. The distance between the skin surface and the femoral artery in the groin area is subject to variation, particularly in relation to the patient's body mass index (BMI). In individuals of normal weight for their height, the femoral artery usually resides 2 to 3 cm below the skin. For those with obesity, the artery can be positioned as deep as 4 cm.

Fig. 11 shows a simplified model that treats the skin and adipose tissues together as a homogeneous material, assuming a uniform optical property for both. Given

that the bevel tip of the needle consistently points upward during insertion, once the needle tip penetrates the tissue, the light emitted from it travels through the tissue and generates a scattering image on the skin's surface. Moreover, we assume that the tissue surface is flat.

The Bouguer-Beer-Lambert law, an exponential function, governs the intensity of the light as it travels through the tissue, causing it to attenuate. We further denote the light intensity emitting from the needle tip as I_0. In this case, the intensity at point P_1 can be calculated as follows:

$$I(P_1) = (1 - R_F)\, I_0 \exp(-\mu_t d_1) \qquad (1)$$

where d_1 is the distance between the light source P_0 and P_1, R_F and μ_t represent the diffuse Fresnel reflectance and the attenuation coefficient of tissue respectively.

In addition, the current system set the distance between the tissue surface and the camera's imaging plane, h, as a fixed value. According to Equation 1, the generated scattering imaging on the tissue surface has a unique mapping to the needle tip relative position inside the tissue. Since establishing the correlation between the needle tip position and the produced scattering image is complex, an AI based method is developed.

The system incorporates a custom-designed needle which is created by inserting an optic fiber (M137L02, Thorlabs Inc., US) into the lumen of a 22G needle and then securing the two components with glue. The Thorlabs 880 nm LED is selected as the light source, because the near-infrared (NIR) spectrum has relatively lower absorption rate in tissue compared to visible light, enabling the light to penetrate thicker tissue. Additionally, the selected light source has a power output of about 0.6 mW, which provides sufficient intensity while maintaining safety.

The control and data acquisition system is based on a portable PC (NUC10i7), which manages a micro-controller (Arduino UNO) for toggling the light source on and off. In addition, a camera (ASI178MM, ZWO Co. Ltd., China) is positioned 100

mm above the tissue surface and interfaced with the PC to capture the scattering image.

A TrakSTAR electromagnet (EM) tracking system (NDI Inc., Canada) is employed to track the spatial position of the needle tip, serving as the ground-truth values for supervised learning. The EM sensor system comprises two main components: a coil and an EM sensor. The coil is securely fastened onto the platform, while the EM sensor is affixed to the needle hub. Please note that the EM sensor is only used for acquiring needle tip position to feed the network training, and is not necessary for the actual deployment.

For data collection, the software system is constructed using the Robot Operation System (ROS) framework, which operates on the NUC PC. Additionally, a system with a Threadripper 5965WX CPU and an NVIDIA RTX 6000 Ada Generation GPU is used for training the AI algorithm which is developed based on PyTorch with PyTorch Lightning. After the AI model has been fully trained, it is tested on the NUC PC to assess its efficacy and performance. We choose to implement the final system on the NUC PC for consideration of system portability.

The calibration procedure comprises two essential steps.
Firstly, the intrinsic parameters of the camera should be acquired in order to generate a distortion-free imaging. This is done by utilizing a chessboard pattern to ensure accurate mapping between real-world coordinates and their corresponding image coordinates. OpenCV lib is employed for calculating these required camera parameters.

Secondly, a coordinate transformation is performed to establish a mapping between the coordinate of the needle tip {N} in relation to the global coordinate on the platform {G}. This task is accomplished through the EM sensor, whose relative position in relation to the coil T_{EM}^{Coil}

EM can be obtained directly. A pivot calibration is done by manually controlling the needle tip to the origin of {G} multiple times and at varying orientations. By collecting a series of data, we can retrieve the relation between the EM sensor and the needle tip, namely T_N^{EM}. Subsequently, the needle tip is navigated to 9

predefined points on the platform, arranged in 3 rows and 3 columns and spaced 30 mm apart. The center of these 9 points is the origin of {G}. The least square method is used to fit the collected points, and we can calculate the transformation matrix between the coil frame and the global frame as T_{Coil}^{G}. The parameter fitting procedure also calculate the residual which corresponds to the Euclidean distance reprojection error of 0.64 mm. With the above transformation matrix obtained, the position of the needle tip in the global coordinate system can be calculated as follows:

$$\mathbf{T}_{N}^{G} = \mathbf{T}_{Coil}^{G} \cdot \mathbf{T}_{EM}^{Coil} \cdot \mathbf{T}_{N}^{EM} \quad (2)$$

AI based Needle tip tracking

Data acquisition

To acquire the required data for training and validating the proposed system, a software system is designed following the workflow illustrated in Fig. 11. This system runs in a loop, and controls the activation and deactivation of the light source during data acquisition process. Images are taken with the needle light on (Img_{on}) continuously only interrupted by an ambient light image (Img_{off}) taken every 2 s with the needle light off. With the use of the newest ambient light image, each illuminated image ambient light can be removed with $Img_{res} = Img_{on} - Img_{off}$. The residual image Img_{res} is then published to the ROS network.

During the data acquisition, the user presses a button on the keyboard and the system automatically save the residual image (downscaled to 400x400) and the current needle tip position with respect to the global coordinate.

Data normalization

In the context of neural networks receiving images as input, each image is divided by the maximum pixel value to enhance convergence for the model. The images are initially stored in a uint16 format, with a pixel value range spanning from 0 to 65535. Consequently, the images are normalized to a range of [0, 1].

Moreover, the 3D positional information corresponds to a spatial region within the global coordinate system. To ensure consistent data representation, the positional

data in the X and Y axes are further normalized to the range of [-1, 1], while the Z-axis data is normalized to the range of [0, 1].

Quaternion processing

Quaternion is used in this invention to represent orientation of the needle tip. Due to the unit norm constraint, the direct probabilistic modelling of quaternion trajectories becomes intractable. For this, we use the method for converting quaternion into Euclidean space. An auxiliary quaternion q_0 is introduced, and a 4-D quaternion q_1 can be transformed to a 3-D vector by calculating the logarithm of orientation difference as follows:

$$\zeta(q_1) = \log(q_1 * q_0) = \begin{cases} \arccos v \frac{\mathbf{u}}{\|\mathbf{u}\|} & \text{if } \mathbf{u} \neq 0 \\ [0\ 0\ 0]^T & \text{if } otherwise. \end{cases} \quad (3)$$

where v and u represent the real and imagine part of q_1 respectively.
To recover the quaternion given the 3-D Euclidean representation (q_2), an exponential operation is conducted.

$$q_2 = \exp(\zeta(q_2)) * q_0 \quad (4)$$

Where

$$\exp(\zeta) = \begin{cases} \cos(\|\zeta\|) + \sin(\|\zeta\|) \frac{\zeta}{\|\zeta\|} & \text{if } \zeta \neq 0 \\ 1 + [0\ 0\ 0]^T & \text{if } otherwise. \end{cases} \quad (5)$$

NTT algorithm architecture

The present invention utilizes a Convolutional Neural Network (CNN) model for processing input images. The CNN architecture chosen for this purpose consists of five convolutional blocks, each employing a varying number of filters: 8, 16, 32, 64, and 128. Each block comprises two convolutional layers that employ Rectified Linear Unit (ReLU) activation function. Following the convolutional layers, a max pooling layer is employed to down sample the feature map. As a result, the final feature map dimensions are 128X4X4. To facilitate further processing, a fully connected layer with 417 neurons, activated by ReLU, is incorporated. The output

layer of the model consists of two fully connected layers with linear activation, which yield predictions for both needle position and orientation. A visual representation of the model architecture can be seen in Fig. 12.

Experiments

Two experiments were designed to evaluate the proposed NTT system and algorithm. The first experiment was based on a rubber phantom which is made of homogeneous material. Specifically, we were dedicated to test and compare the system performances with different exposure times. Furthermore, the second experiment was carried out on a more realistic porcine phantom. By employing this sequential approach, the experimental design aims to validate the proposed method in guiding needle insertion during the femoral artery intravenous task. Also, the test is conducted to evaluate the proposed method's potential in other medical applications that involve more intricate anatomical structures.

The evaluation metrics include positional accuracy, orientation accuracy and processing time. The orientation accuracy is quantified by the absolute value $||\zeta||$ using Equation 3 with q_0 as the ground-truth value and q_1 as the predicted value.

Preliminary experiment on rubber phantom

The first experiment was conducted on a TruIV block phantom (Limbs & Things Co., UK), which is made of homogeneous rubbery material. During the experiment, the optic needle was manually inserted into the phantom in various depths and orientations for generating datasets. Specifically, the data were collected within a box with a length of 60 mm, a width of 40 mm and a depth of 45 mm. The insertion angle was kept with the needle bevel tip facing up towards the camera. The pitch φ was between 30° and 70° with a yaw θ from -45° to 45°. The data collection process was conducted with even sampling across the defined space.

In total, two datasets were generated, comprising images and the corresponding spatial position of the needle tip in 6-DOFs. One dataset was captured with an exposure time of 20 ms, while the other dataset utilized an exposure time of 100 ms with 511 samples each.

The dataset was divided into three subsets using a 60/20/20 split, where 60% of the data was allocated for training, 20% for validation, and the remaining 20% for testing.

System evaluation based on porcine phantom

The second set of experiments involved the use of porcine tissue phantoms to create a realistic evaluation environment. For this purpose, two types of phantoms were obtained from the market: a piece of bacon and a piece of fresh pork slab. The size of both phantoms were big enough for ensuring coverage of the camera's field of view. The bacon phantom featured a 2 mm thick layer of skin and a substantial layer of fat, closely simulating the actual anatomical characteristics of the human groin area. The total thickness of the bacon phantom was measured to be 34.9±2.2 mm. As for the fresh pork phantom, a more complicated anatomic structure was observed with intersecting layers of fat and muscle beneath the skin surface. The overall thickness of the fresh pork phantom was found to be 47.8±3.2 mm. This complex anatomical structure allows us to assess the capabilities of the proposed technology in handling more intricate medical applications.

During the experiment, one of the phantom was placed on the platform, and then, the camera height was adjusted to maintain a distance of 100 mm above the tissue surface. Following this setup, a data collection procedure similar to the one employed in the first experiment was conducted, but only 100 ms exposure time was used. This was because a far better performance was received from the experiments on the rubber phantom. During the data collection, the needle was manually inserted into the tissue at various depths and angles, encompassing a range identical to that of the first experiment. Care was taken to ensure a straight needle shaft before proceeding with data recording, including both the scattering image Img_{res} and the corresponding needle tip position.

In the second experiment, a dataset of 1367 samples on bacon and 1142 samples on fresh was created. The data processing was the same as in the first experiment. The data were divided into a 60/20/20 split for the training, validation, and test dataset. The collected data from the second experiment were utilized to train the proposed CNN-based model. The previously identified

hyperparameters found effective for the phantom model were applied in this training process.

Model training and hyperparameter tuning

In order to determine the optimal parameters for the model's architecture and training, a Bayesian hyperparameter tuning approach was employed with the training and validation split from the rubber phantom. The ranges of the explored parameter values can be found in Table 1. During the model's training process, a learning rate scheduler was employed if the hyperparameter was true. This scheduler would reduce the current learning rate with a factor of 0.1 if the validation loss of the model did not demonstrate improvement within a span of 30 epochs and terminates the training if no improvement is seen within 100 epochs. The loss function used for the model training is a Mean Squared Error (MSE) loss with the position and orientation $Loss = MSE_p(p, \hat{p}) + a \cdot MSE0(o, \hat{o})$, where p and o is the ground-truth position and orientation vectors p = [x y z], o = [o_x o_y o_z], $\hat{p}$ and $\hat{o}$ the model prediction for the position and orientation and a being the loss weight for the orientation. The Bayesian hyperparameter tuning used the best validation loss score for the parameter search.

Table 1: Parameter ranges for hyperparameter tuning

Parameter	**Range**	
Optimizer	Adam, AdamW, SGD	
Batch Size	4	64
Conv Blocks (CB)	1	5
CB initial filter	4	16
Fully Connected layers	1	4
Fully Connected Layer Size	10	512
Use learning rate schedule	Yes	No
Loss weight orientation	0.0,	1.0
Learning Rate	1e-9	1e-1

The following parameter settings were selected from 668 runs: the AdamW optimizer, with a batch size 32. The initial filter count for the convolutional blocks was set to 8 with 5 blocks, while the fully connected layer had a size of 517 neurons with one layer. The learning rate was set to 0.00013 with a learning rate scheduler. The orientation component of the loss was weight with 1.174.

Results based on the rubber phantom

Table 2 presents the computed position accuracy in the X, Y, and Z components, as well as the L2 norm, based on the test set. For each component, the mean error, standard deviation (STD) and 90 percentile (90%ile) are reported. To mitigate the influence of random weight initialization, the models were trained independently ten times, and the aggregated results were considered for analysis.

The results in Table 2 indicate that small differences of the position accuracy in the X, Y, and Z component. Additionally, results using 100 ms exposure time are found considerably better compared to the results using 20 ms exposure time. Moreover, the L2 norm errors in different insertion depths Z* are plotted in Fig. 13. The insertion depth Z* is obtained by subtracting the needle tip's Z value, relative to the global coordinate, from the height of the phantom. Relatively higher errors are observed from the first 5 mm of depth, while

Table 2: The mean error (mean), standard deviation (STD) and 90 percentile (90%ile) in mm comparing the CNN output and ground-truth on the rubber phantom with 20 and 100 ms exposure time based on the test set.

	mean		STD		90th %ile	
Exposure	20	100	20	100	20	100
X	1.7	1.1	2.6	1.0	3.5	2.7
Y	3.5	1.2	2.8	1.3	7.4	2.3
Z	1.5	1.1	1.9	1.0	3.2	2.4
L2	4.7	2.3	3.6	1.5	9.1	3.9

Table 3: The orientation error obtained from the rubber phantom experiment.

	mean		STD		90th %ile	
Exposure	20	100	20	100	20	100
$\|\|\zeta\|\|$	0.24	0.20	0.14	0.11	0.5	0.4

The results from 5 to 40 mm are found relatively consistent. Also, higher positional accuracy of the system with 100 ms exposure time is found compared to that with 20 ms exposure time.

The orientation accuracy, presented as $||\zeta||$, are presented in table 3. Results of different exposure time, namely 20 ms and 100 ms, are shown together for comparison.

Results based on porcine phantoms

The positional tracking error based on the bacon and fresh porcine phantoms are summarized in Table 4. Specifically, the errors in the X, Y, and Z directions, as well as their corresponding L2 norm are presented. The observed errors in the X, Y, and Z component exhibits similarities: approximately 1.0 mm for the bacon phantom and 1.6 mm for the fresh pork phantom. In fact, the tracking accuracy (L2 norm) is higher for the bacon phantom compared to the fresh pork phantom, with values of 2.0±1.2 mm and 3.2±3.1 mm respectively.

The L2 norm accuracy in different insertion depths Z^* are shown in Figure 8. The errors observed in the results obtained from the bacon phantom are relatively smaller when compared to those from the fresh pork phantom. This is coherent to the results reported in Table 4. In addition, the results collected from the bacon phantom demonstrate consistency across different insertion depths. In contrast, an increasing trend is evident in the results acquired from the fresh pork phantom. In addition, the needle tip orientation tracking errors are provided in Table 5. Slightly higher accuracy in tip orientation estimation is found on the bacon phantom (0.16±0.1) compared to the fresh pork phantom (0.19±0.1).

Processing time

The proposed system and the CNN based tracking algorithm was implemented and tested on a portable PC, NUC (Intel i7 CPU). In addition to the camera's frame rate, the processing time was found to be 20.2±0.8 ms. Notably, the processing time can be further reduced to sub-millisecond when the same algorithm was tested on a computer with graphical processing units (GPUs). This observation suggests that the proposed system is sufficiently fast for real-time tracking of the needle tip, even when implemented on a portable setup.

Discussion

Through a comparison of the results obtained from the rubber phantom, it is evident that the positional error with a 20 ms exposure time (4.7±3.6 mm)

Table 4: The mean error (mean), standard deviation (STD) and 90 percentile (90%ile) in mm comparing the CNN output and ground-truth on both the bacon phantom (Bacon) and the fresh pork phantom (Fresh) based on the test set.

	mean		STD		90th %ile	
Phantom	Bacon	Fresh	Bacon	Fresh	Bacon	Fresh
X	0.9	1.5	0.8	2.0	2.0	3.1
Y	1.0	1.6	0.8	2.4	2.0	3.2
Z	1.2	1.6	1.0	1.4	2.5	3.4
L2	2.0	3.2	1.2	3.1	3.6	5.4

Table 5: Orientation error of needle tip tracking results on the bacon phantom (Bacon) and the fresh pork phantom (Fresh).

	mean		STD		90th %ile	
Phantom	Bacon	Fresh	Bacon	Fresh	Bacon	Fresh
$\|\|\zeta\|\|$	0.16	0.19	0.10	0.10	0.3	0.3

is higher than that with a 100 ms exposure time (2.3±1.5 mm). These findings highlight the significance of exposure time as a key factor in generating adequate intensity on the tissue surface, particularly when the needle is inserted to depths of up to 40 mm. Nevertheless, an alternative approach to enhance lighting intensity can be through increasing the power of the light source.

Based on the results obtained from the porcine experiment, the L2 norm errors derived from the bacon phantom remained within 3.6 mm, whereas the errors from the fresh pork phantom are generally higher, mostly within 5.4 mm. In fact, the bacon phantom more closely resembles the anatomy of the human groin area, where mostly consists of fat. Therefore, the achievement of a 3.6 mm error demonstrates the efficacy of the proposed technology, considering that the radius of the femoral artery typically ranges from 4 to 5 mm. Also, the proposed method is considered sufficient for this application since only the tracking accuracy in X and Y direction are more critical to target the needle to the artery.

The results obtained from the fresh pork phantom exhibit reasonable performance up to an insertion depth of 30 mm. However, the errors noticeably escalate from $Z^* = 30$ mm to 40 mm, as shown in Figure 8. This occurrence can be attributed to the significant reduction in light intensity captured by the camera. In Fig. 15, examples of imaging from two different depths (10 mm and 30 mm) for both the bacon and fresh pork phantoms are provided. It is evident that the lighting intensity for the fresh pork phantom at $Z^* = 30$ mm becomes hard to discern, whereas the lighting from the needle tip at the same depth remains distinguishable for the bacon phantom. This can be interpreted due to the higher concentration of muscle in the fresh pork phantom, which absorbs a greater amount of light (near-infrared), affecting the intensity of the captured images. Given the tracking error within 5.4 mm, the proposed system is still demonstrated to be able for easy extension to various medical applications with more complex anatomical features.

Furthermore, we can see that a slightly higher error is observed for $Z^* <= 5$mm in the results obtained from the rubber phantom (Fig. 13). This discrepancy is suspected to be caused by the insufficient number of samples collected near the surface of the phantom. To avoid this, an additional 100 samples were collected from the near-surface $Z^* <= 10$mm during the experiments conducted on the bacon and the fresh pork phantoms. Consequently, it is found that the error in the near-surface area is not higher than that in the subsurface region, as shown in Fig. 14.

It is also interesting to see that the darkened skin of the bacon phantom surprisingly does not excessively hinder the passage of light. As a result, the camera is still able to capture high-intensity images even at greater insertion depths. This finding is encouraging as it suggests that the system possesses robust potential for use across different skin tones.

In this invention, the accuracy of needle orientation tracking is measured by the $||\zeta||$ value, which ranges from 0 to π, with smaller values indicating higher accuracy. The results demonstrate that the orientation accuracy achieved is commendable. While it may not be critical for this specific application, the ability

to track needle orientation holds significant importance in other medical applications, such as needle steering.

The power of the light source has not been optimized. For safety considerations, an ultra-low power light source (0.6 mW) is chosen. However, it is possible to utilize a relatively higher power light source. In this case, it would be feasible to reduce the exposure time of the camera while maintaining a comparable level of imaging quality. Secondly, despite our efforts to ensure a straight needle shaft during data collection, small manual errors may still involve, affecting the consistency of the transformation matrix between the needle tip and the EM sensor. While these errors are challenging to completely eliminate, multiple measures were taken to minimize their impact. Additionally, the above positional accuracy in each case must be assessed in relation to the system's calibration. Namely, the Euclidean distance reprojection error, 0.64 mm, should be taken into account when evaluating the system's performance. Also, to use this method in practise, virtual reality technique can be integrated in the future for guiding the whole insertion process.

It is to be understood, that guiding is to be construed as the provision of spatial information relating to the surgical instrument.

This invention presents a cutting-edge technology aiming to achieve precise and efficient needle tip tracking during the insertion to a deep subsurface location. The system is developed through combining optical imaging and AI-based algorithms. Experimental evaluations conducted on rubber and porcine tissue phantoms validate the system's capability for accurate and real-time tracking of the needle tip during the insertion procedure. In addition, the results highlight the potential of the system to enhance the safety and efficiency of femoral artery insertion procedures, and demonstrate its versatility for different medical applications.

Fig. 16 shows a graph, the graph representing a performance study perform in relation to different image resolutions.

A study was conducted on the impact of image resolution on the performance of a Convolutional Neural Network (CNN) for needle tracking. In this study, the researchers compared the performance of the CNN using original images with

those resized to different dimensions. The original images were of size 400x400 pixels, while the resized versions were 8, 16, 32, and 64 pixels. The performance is evaluated as the error in mm between the needle tracking sensor (ground truth) and the model estimate for the 3 coordinates x,y,z. Two sets of samples were utilized in the study: one for training, consisting of nearly 800 images, and another for testing, comprising over 200 images.

The results are shown in the following figure, with performance, as difference in mm compared between true measured and determined by the CNN, shown on y-axis; and resolution in pixels shown on the x-axis. The performance improves from 8x8 pixels to 32x32 pixels. Beyond this point, however, additional information does not yield further improvement in model performance, leading to a plateau effect.

From this study, the inventors were able to determine that an optimal array of sensors for a patch is between 32x32 and 128x128 sensors.

Fig. 17 shows a confusion matrix CONF MAT., related to puncture detection accuracy, based on a study performed on tissue (fat from a pig) and fake blood respectively, using the algorithm according to the invention, to detect a change between a first and second tissue. T. indicates true value and PRED. indicates predicted by the algorithm.

The algorithm performed with the following accuracy:

Recall: 72%

Specificity: 98%

F1-score: 88%

Precision: 79%

Accuracy: 93%

Thus, the inventors has demonstrated that the algorithm provides a high accuracy in determining a change in tissue, from at least between fat and blood.

It is to be understood, that a confusion matrix, is a tool for evaluating the performance of a machine learning model, especially in classification tasks.

True Positives (TP):

These occur when the model accurately predicts a positive data point.
For instance, if our model correctly identifies a relevant event (where "positive" represents the occurrence of the event), it's a true positive.
True Negatives (TN):
These occur when the model accurately predicts a negative data point.
For example, if the model correctly classifies a non-event scenario (where "negative" represents the absence of the event), it's a true negative.
False Positives (FP):
These occur when the model predicts a positive data point incorrectly.
Imagine the model incorrectly labeling a non-event scenario as an event; that's a false positive.
False Negatives (FN):
These occur when the model mispredicts a negative data point.
For instance, if the model fails to identify an actual event, it's a false negative.

The above calculations have been performed in the following manner:

Precision (also called positive predictive value):
Precision measures the proportion of true positive predictions out of all positive predictions made by the model.
It answers the question: "Of all the positive predictions, how many were actually correct?"
Precision = TP / (TP + FP)

Recall (also called sensitivity or true positive rate):
Recall measures the proportion of true positive predictions out of all actual positive instances.
It answers the question: "Of all the actual positive instances, how many did the model correctly predict?"
Recall = TP / (TP + FN)

F1 Score:
The F1 score is the harmonic mean of precision and recall.
It balances precision and recall, especially when one of them is significantly higher than the other.

F1 Score = 2 * (Precision * Recall) / (Precision + Recall)

Further, the researchers performed a study for arterial and venous identification: Two kinds of fake blood (arterial and venous) were tested at two wavelengths, 660nm and 850nm, which were emitted from the surgical instrument.

The study found, that when using 660 nm as lighting source, the system was able to achieve 90% accuracy in classifying artery and vein.

When 850 nm light source was used, 81% accuracy for this classification was achieved.

In short, the invention relates to a system and method for providing the depth and orientation of a surgical instrument inserted into biological tissue. The system comprises a surgical instrument adapted to emit light into the biological tissue and a light detection device outside said tissue, and wherein an algorithm is adapted to provide said depth and orientation information, based on light scatter detected by the light detection device; and a peripheral user interface adapted to receive and display said information to a user if the surgical instrument, such as a health care person. In particular, the invention is advantageous for aiding e.g. a nurse in reaching a small blood vessel of e.g. an infant or small child with a cannula. Further, the invention is advantageous for training health care personnel to improve their needle insertion technique, such as with a training phantom and provide decision support during needle insertion.

Although the present invention has been described in connection with the specified embodiments, it should not be construed as being in any way limited to the presented examples. The scope of the present invention is set out by the accompanying claim set. In the context of the claims, the terms "comprising" or "comprises" do not exclude other possible elements or steps. Also, the mentioning of references such as "a" or "an" etc. should not be construed as excluding a plurality. The use of reference signs in the claims with respect to elements indicated in the figures shall also not be construed as limiting the scope of the invention. Furthermore, individual features mentioned in different claims, may possibly be advantageously combined, and the mentioning of these features in

different claims does not exclude that a combination of features is not possible and advantageous.

In exemplary embodiments E1-E20 the invention may relate to:

E1. A computer implemented method of determining the spatial position and orientation of a surgical instrument, such as a cannula or catheter, when the surgical instrument is positioned within tissue of a subject, the computer implemented method comprising:
-emitting light from a portion of the surgical instrument at least when said portion is positioned within tissue,
-providing a light detection device outside of said tissue,
-detecting light scatter from within the tissue, with the light detection device,
-providing an algorithm adapted to determine the spatial position and orientation of the instrument, relative to a reference point, into said tissue, based on the light scattered from within the tissue,
-providing the position and orientation of the surgical instrument to a user.

E2. The computer implemented method according to embodiment 1, wherein the algorithm is a machine learning algorithm, the method further comprising:
-providing said machine learning algorithm with a training set adapted to train the machine learning algorithm to determining the position and orientation of the surgical instrument emitting light within a tissue, the training set being based on predetermined spatial positions, orientations and light scatter patterns of light emitted from tissue.

E3. The computer implemented method according to embodiment 1 or embodiment 2, the method further comprising:
-providing light scatter information relating to tissue structures, such as blood vessels, nerves or bone, adjacent to the light emitted from the surgical instrument and providing the user with spatial tissue structure information relative to a current position of the surgical instrument.

E4. The computer implemented method according to any of the preceding embodiments, the method further comprising:

-providing verification to the user relating to the surgical instrument entering a tissue structure, such as a blood vessel, within the tissue, based on the detected light scatter from within said tissue structure.

E5. The computer implemented method according to any of the preceding embodiments, the method further comprising mapping tissue structures adjacent to the instrument, based on the light scatter and providing a spatial overview of the tissue to the user.

E6. The computer implemented method according to any of the preceding embodiments further comprising:

-receiving an input from the user relating to a selected target within the tissue,

-guiding the user to translate the surgical device to said target based on detected light scatter,

and when the surgical instrument is positioned at or within said target,

-verifying the position of the surgical instrument at or within said target to the user.

E7. The computer implemented method according to any of the preceding embodiments, the method further comprising applying graphics processing units (GPU's) to train and perform the machine learning algorithm.

E8. A spatial positioning and orientation system for a surgical instrument, the system comprising:

-a light detection device arranged outside the tissue,

-a user interface in data communication with the light detection device,

-an instrument adapted to emit light from a portion of said instrument within tissue, when said portion of the instrument is positioned within tissue,

-a processor adapted to execute an algorithm, said algorithm determining a spatial position and orientation of the surgical instrument within the tissue, based on light scattered from within the tissue and detected by the light detection device, wherein the system is configured to provide the spatial position and orientation of the surgical instrument to a user through the user interface, while said user operates the surgical instrument within tissue of a subject.

E9. The system according to embodiment E8, wherein the light detection device is a camera positioned at least above an entry point of the tissue, the entry point being the point of entry of the surgical device into the tissue of the subject, the system further comprising a distance measuring device adapted to measure a distance between an outer surface of the tissue and said camera, the device adapted to calibrate the measured light scatter from the tissue to the camera.

E10. The system according to embodiment E8, wherein the light detection device is a sensory array, preferably a patch with an array of sensors, adapted to be adhered to skin of a subject adjacent to an entry point into tissue of said subject, the sensory array comprising photo-sensors adapted to detect light scatter from within said tissue.

E11. The system according to any of embodiments E8, E9 or E10, the surgical instrument comprising one or more light sources, such as an LED or an array of LED's, the light source(s) positioned at or near a distal tip of the surgical instrument.

E12. The system according to any of embodiments E8, E9 or E10, the surgical instrument being adapted with a lumen comprising one or more optical fibres adapted to emit light at or near a distal tip of the surgical instrument.

E13. The system according to any of embodiments E11 or E12, wherein a plurality of light sources is adapted to emit light at different wavelengths and/or or at different temporal intervals, to generate a specific pattern of light emitted.

E14. The system according to any of embodiments E8 to E13, the system being a decision support system and wherein the system is adapted to guide the user to reach a target of the tissue with the surgical instrument, said target being specified by said user through the user interface.

E15. The system according to any of embodiments E8 to E14, the user interface comprising visible or audible output adapted to guide the user to operate the surgical instrument within tissue.

E16. The system according to any of embodiments E8 to E15, wherein the processor applies graphics processing units (GPU's) to train and perform a machine learning algorithm.

E17. The system according to any of embodiments E8 to E16 further comprising a bioimpedance sensor adapted to measure changes in electrical conductivity.

E18. A surgical instrument, preferably cannula, comprising:

-a light source at or near a distal tip of the instrument,

-a light detection device at a proximal location of the instrument,

-a processor adapted to receive and process a signal received from the light detection device,

-a wireless transmitter adapted to transmit processed data from the processor to an associated peripheral device, such as a computer, and

-optionally an energy storage device, such as a battery,

wherein the surgical instrument is configured to detect light scatter from within tissue, when at least the distal tip of the surgical device is inserted into said tissue and provide information relating to tissue structures adjacent to the light source, to a user through said associated peripheral device.

E19. The surgical instrument according to E18, further comprising a bioimpedance sensor adapted to measure changes in electrical conductivity.

E20. The surgical instrument according to E19, wherein the bioimpedance sensor is integrated into or near the distal tip of the instrument.

E21. The computer implemented method according to any of embodiments E1 to E7 further comprising:

-receiving an input from the user relating to a selected target within the tissue,

-providing a current position and orientation of the surgical instrument to the user;

and when the surgical instrument has been positioned at or within said target,

-verifying the position of the surgical instrument at or within said target to the user.

E22. The computer implemented method according to any of embodiments E1 or E3 to E6, wherein the algorithm is selected from one or more of a convolutional neural network or fundamental image processing in combination with multi-layer perceptron.

E23. The computer implemented method according to E1, the method further comprising

-detecting a first tissue based on the light scatter,

-detecting a second tissue based on a change in the light scatter,

-providing the user with information that a second tissue has been detected.

E24. The system according to any of embodiments E10 to E17, wherein the sensory array comprises at least 8x8 sensors, preferably at least 16x16 sensors, even more preferred at least 32x32 sensors.

E25. The system according to any of embodiments E10 to E17, wherein the sensory array comprises between 32x32 and 128x128 sensors.

E26. A method of training an algorithm to determine the spatial position and orientation of the surgical instrument according to any of embodiments E18 to E20, the training method comprising:

-providing the algorithm with a training set adapted to train the algorithm to determine the position and orientation of the surgical instrument emitting light within a tissue, the training set being based on predetermined spatial positions, orientations and light scatter patterns of light emitted from tissue.

E27. The method of training an algorithm according to E26, wherein the training set comprises at least a first set of images obtained from outside of the tissue,

and a data set comprising a measured position and orientation of the surgical instrument within the tissue.

E28. The method of training an algorithm according to any of embodiments E26 or E27, wherein the algorithm is further trained to detect the transition of position of the surgical instrument, from a first tissue to a second tissue.

E29. The method of training an algorithm according to any of embodiments E26 to E28, wherein the training set further comprises images obtained from outside of the tissue, wherein the surgical instrument emits light within the first tissue, and images wherein the surgical instrument emits light within the second tissue, training the algorithm to detect a change in tissue.

E30. The method of training an algorithm according to any of embodiments E26 to E29, wherein the algorithm is selected from one or more of a convolutional neural network or fundamental image processing in combination with multi-layer perceptron.

E31. The surgical instrument according to any of embodiments E18 to E20, wherein the light source is an optic fiber provided through a lumen of said surgical instrument.

E32. The surgical instrument according to any of embodiments E18 to E20 or E31, wherein the light source is adapted with a lens.

E33. The computer implemented method according to any of the embodiments E1 to E7 or E21 to E23, wherein the emitted light is adapted with a spatial pattern.

E34. The computer implemented method according to any of the embodiments E1 to E7 or E21 to E23, wherein the emitted light is adapted with a temporal pattern.

E35. The computer implemented method according to any of the embodiments E1 to E7 or E21 to E23, wherein the emitted light is adapted with a spatial pattern and temporal pattern.

E36. The computer implemented method according to any of the embodiments E1 to E7 or E21 to E23 or E33 to E35 further comprising

-emitting light from at least a second portion of the surgical instrument and wherein at least one of the emitted lights are adapted with a temporal or spatial pattern.

CLAIMS

1. A computer implemented method of determining the spatial position and orientation of a surgical instrument, such as a cannula or catheter, when the surgical instrument, prior to the method, is positioned within tissue of a subject, the computer implemented method comprising:
-emitting light from a portion of the surgical instrument at least when said portion is positioned within tissue,
-providing a light detection device outside of said tissue,
-detecting light scatter from within the tissue, with the light detection device,
-providing an algorithm adapted to determine the spatial position and orientation of the instrument, relative to a reference point, into said tissue, based on the light scattered from within the tissue,
-providing the position and orientation of the surgical instrument to a user.

2. The computer implemented method according to claim 1, wherein the algorithm is a machine learning algorithm, the method further comprising:
-providing said machine learning algorithm with a training set adapted to train the machine learning algorithm to determining the position and orientation of the surgical instrument emitting light within a tissue, the training set being based on predetermined spatial positions, orientations and light scatter patterns of light emitted from tissue.

3. The computer implemented method according to claim 1 or claim 2, the method further comprising:
-providing light scatter information relating to tissue structures, such as blood vessels, nerves or bone, adjacent to the light emitted from the surgical instrument and providing the user with spatial tissue structure information relative to a current position of the surgical instrument.

4. The computer implemented method according to any of the preceding claims, the method further comprising:
-providing verification to the user relating to the surgical instrument having entered a tissue structure, such as a blood vessel, within the tissue, based on the detected light scatter from within said tissue structure.

5. The computer implemented method according to any of the preceding claims, the method further comprising mapping tissue structures adjacent to the instrument, based on the light scatter and providing a spatial overview of the tissue to the user.

6. The computer implemented method according to any of the preceding claims further comprising:

-receiving an input from the user relating to a selected target within the tissue,

-providing a current position and orientation of the surgical instrument to the user;

and when the surgical instrument has been positioned at or within said target,

-verifying the position of the surgical instrument at or within said target to the user.

7. The computer implemented method according to any of claims 1 or 3 to 6, wherein the algorithm is selected from one or more of a convolutional neural network or fundamental image processing in combination with multi-layer perceptron.

8. The computer implemented method according to claim 1, the method further comprising

-detecting a first tissue based on the light scatter,

-detecting a second tissue based on a change in the light scatter,

-providing the user with information that a second tissue has been detected.

9. The computer implemented method according to any of the preceding claims, wherein the emitted light is adapted with a spatial pattern.

10. The computer implemented method according to any of the preceding claims, wherein the emitted light is adapted with a temporal pattern.

11. The computer implemented method according to any of the preceding claims, wherein the emitted light is adapted with a spatial pattern and temporal pattern.

12. The computer implemented method according to any of the preceding claims further comprising
-emitting light from at least a second portion of the surgical instrument and wherein at least one of the emitted lights are adapted with a temporal or spatial pattern.

13. A spatial positioning and orientation system for a surgical instrument, the system comprising:
-a light detection device arranged outside the tissue,
-a user interface in data communication with the light detection device,
-an instrument adapted to emit light from a portion of said instrument within tissue, when said portion of the instrument is positioned within tissue,
-a processor adapted to execute an algorithm, said algorithm determining a spatial position and orientation of the surgical instrument within the tissue, based on light scattered from within the tissue and detected by the light detection device, wherein the system is configured to provide the spatial position and orientation of the surgical instrument to a user through the user interface, while said user operates the surgical instrument within tissue of a subject.

14. The system according to claim 3, wherein the light detection device is a camera positioned at least above an entry point of the tissue, the entry point being the point of entry of the surgical device into the tissue of the subject, the system further comprising a distance measuring device adapted to measure a distance between an outer surface of the tissue and said camera, the device adapted to calibrate the measured light scatter from the tissue to the camera.

15. The system according to claim 13, wherein the light detection device is a sensory array, preferably a patch with an array of sensors, adapted to be adhered to skin of a subject adjacent to an entry point into tissue of said subject, the sensory array comprising photo-sensors adapted to detect light scatter from within said tissue.

16. The system according to any of claims 13, 14 or 15, the surgical instrument comprising one or more light sources, such as an LED or an array of LED's, the light source(s) positioned at or near a distal tip of the surgical instrument.

17. The system according to any of claims 13, 14 or 15, the surgical instrument being adapted with a lumen comprising one or more optical fibres adapted to emit light at or near a distal tip of the surgical instrument.

18. The system according to any of claims 16 or 17, wherein a plurality of light sources is adapted to emit light at different wavelengths and/or or at different temporal intervals, to generate a specific pattern of light emitted.

19. The system according to any of claims 13 to 18, the system being a decision support system and wherein the system is adapted to guide the user to reach a target of the tissue with the surgical instrument, said target being specified by said user through the user interface.

20. The system according to any of claims 13 to 19, the user interface comprising visible or audible output adapted to guide the user to operate the surgical instrument within tissue.

21. The system according to any of claims 15 to 20, wherein the sensory array comprises at least 8x8 sensors, preferably at least 16x16 sensors, even more preferred at least 32x32 sensors.

22. The system according to any of claims 15 to 20, wherein the sensory array comprises between 32x32 and 128x128 sensors.

23. A surgical instrument, preferably cannula, comprising:

-a light source at or near a distal tip of the instrument,

-a light detection device at a proximal location of the instrument,

-a processor adapted to receive and process a signal received from the light detection device,

-a wireless transmitter adapted to transmit processed data from the processor to an associated peripheral device, such as a computer, and

-optionally an energy storage device, such as a battery,
wherein the surgical instrument is configured to detect light scatter from within tissue, when at least the distal tip of the surgical device is inserted into said tissue and provide information relating to tissue structures adjacent to the light source, to a user through said associated peripheral device.

24. The surgical instrument according to claim 23, further comprising a bioimpedance sensor adapted to measure changes in electrical conductivity.

25. The surgical instrument according to claim 24, wherein the bioimpedance sensor is integrated into or near the distal tip of the instrument.

26. The surgical instrument according to any of claims 23 to 25, wherein the light source is an optic fiber provided through a lumen of said surgical instrument.

27. The surgical instrument according to any of claims 23 to 26, wherein the light source is adapted with a lens.

28. A method of training an algorithm to determine the spatial position and orientation of the surgical instrument according to any of claims 23 to 27, the training method comprising:
-providing the algorithm with a training set adapted to train the algorithm to determine the position and orientation of the surgical instrument emitting light within a tissue, the training set being based on predetermined spatial positions, orientations and light scatter patterns of light emitted from tissue.

29. The method of training an algorithm according to claim 28, wherein the training set comprises at least a first set of images obtained from outside of the tissue, and a data set comprising a measured position and orientation of the surgical instrument within the tissue.

30. The method of training an algorithm according to any of claims 28 or 29, wherein the algorithm is further trained to detect the transition of position of the surgical instrument, from a first tissue to a second tissue.

31. The method of training an algorithm according to any of claims 28 to 30, wherein the training set further comprises images obtained from outside of the tissue, wherein the surgical instrument emits light within the first tissue, and images wherein the surgical instrument emits light within the second tissue, training the algorithm to detect a change in tissue.

32. The method of training an algorithm according to any of claims 28 to 31, wherein the algorithm is selected from one or more of a convolutional neural network or fundamental image processing in combination with multi-layer perceptron.

33. The computer implemented method according to claim 1 or the system according to claim 13 or the surgical instrument according to claim 23 or the method of training according to claim 28, wherein the light is emitted at a wavelength of between 600 and 900 nm, preferably between 660 and 850 nm.

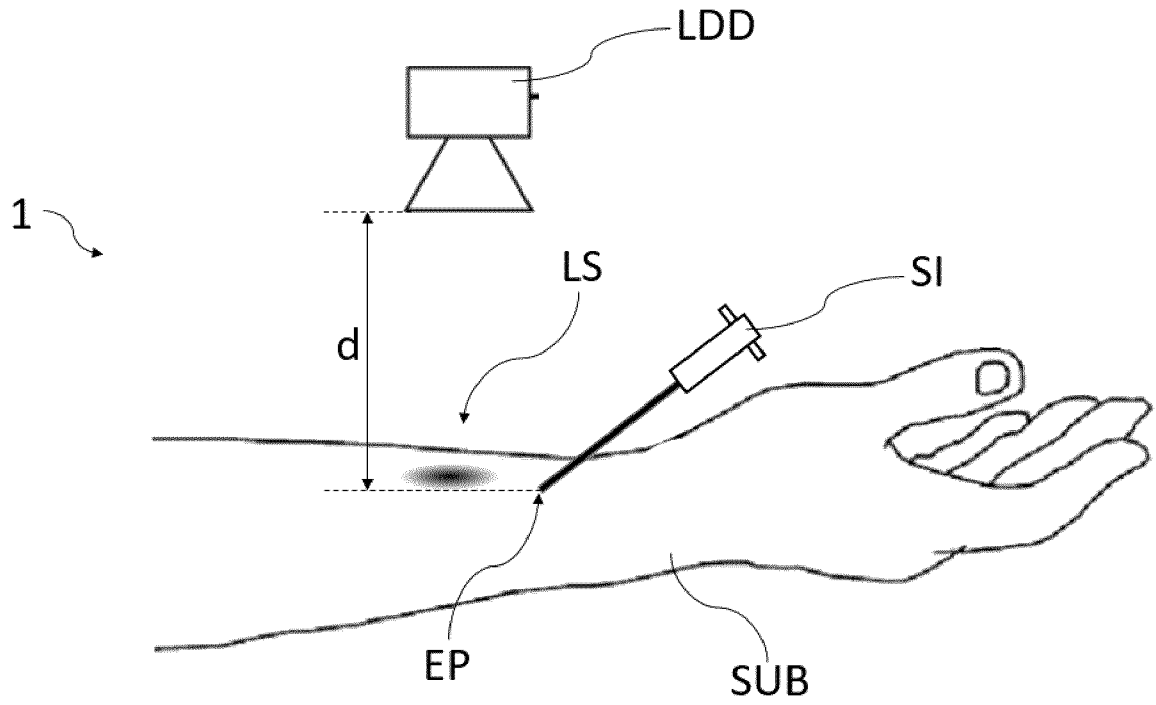

Fig. 1

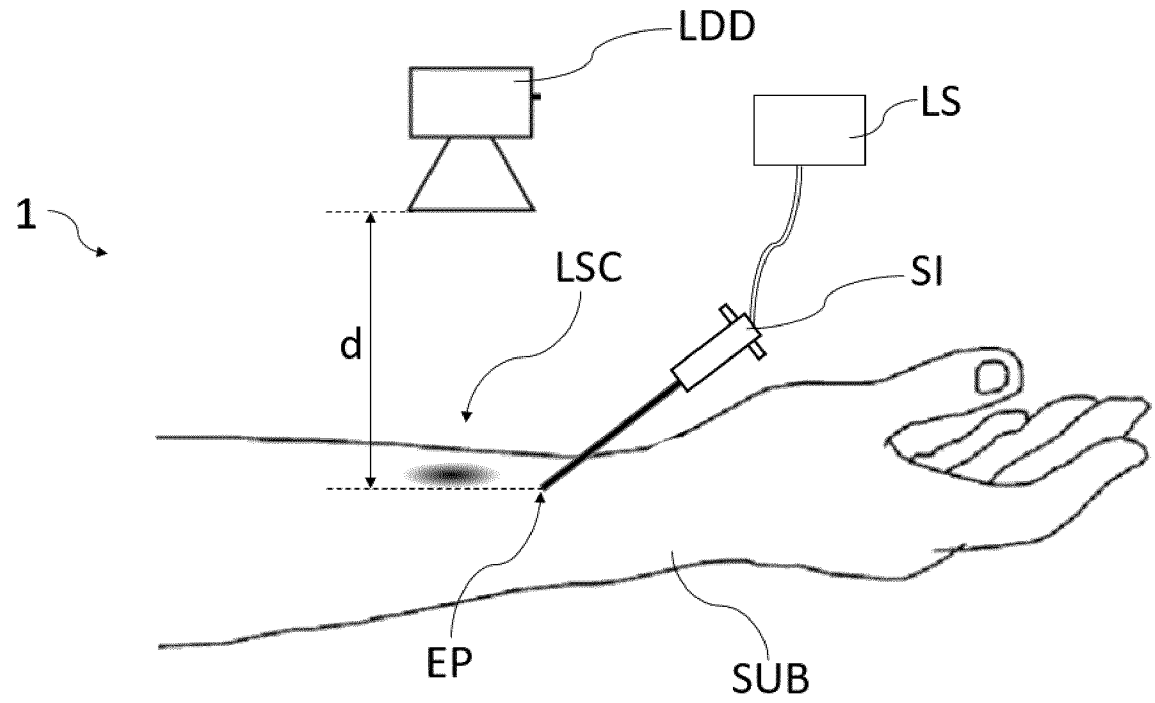

Fig. 2

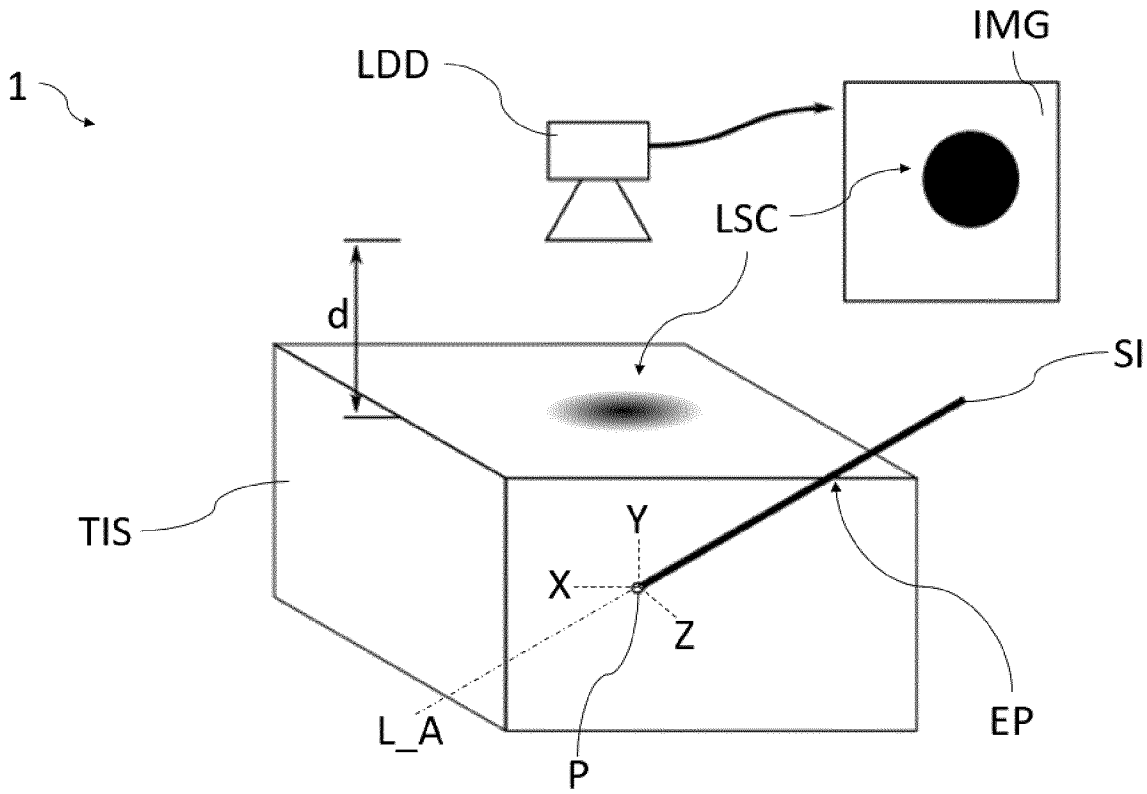

Fig. 3

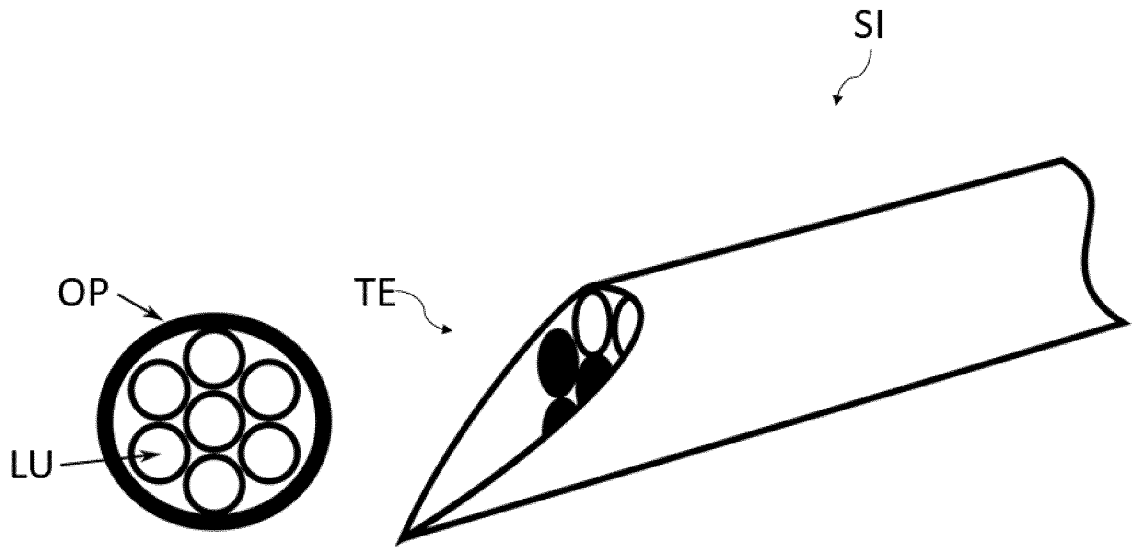

Fig. 4

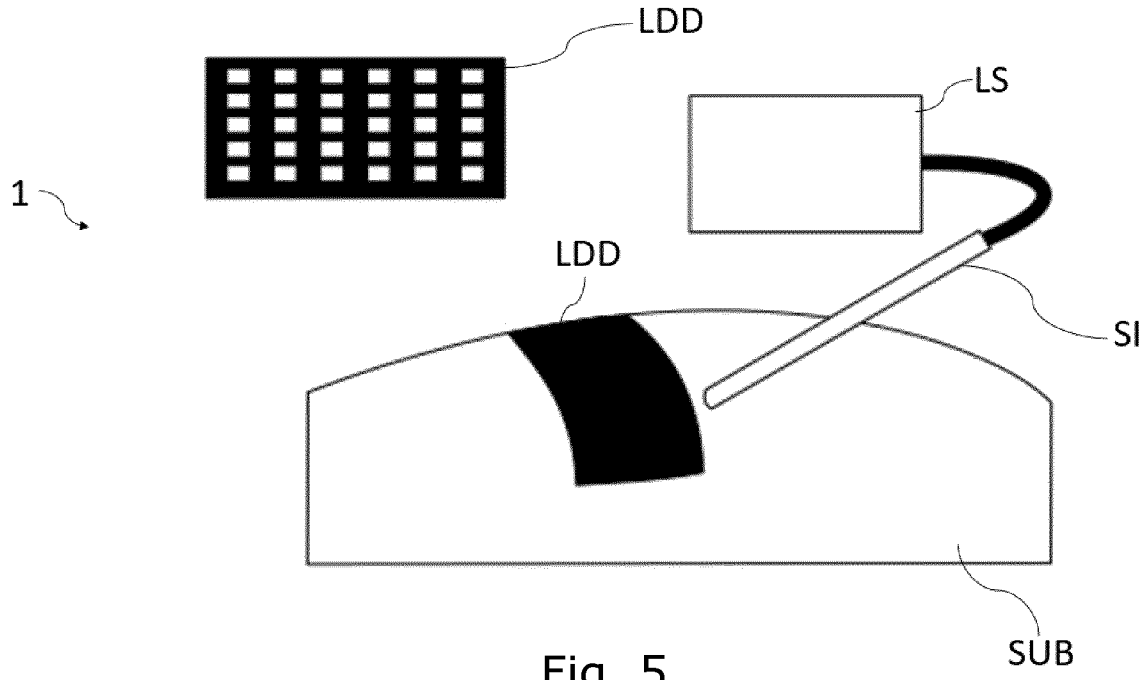

Fig. 5

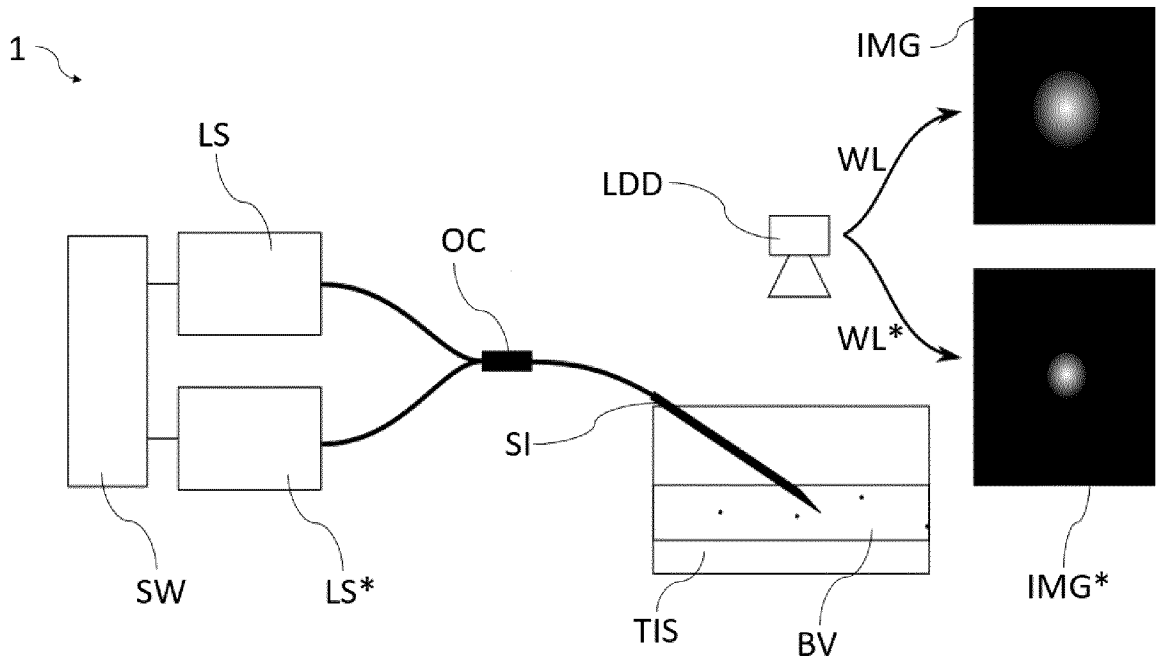

Fig. 6

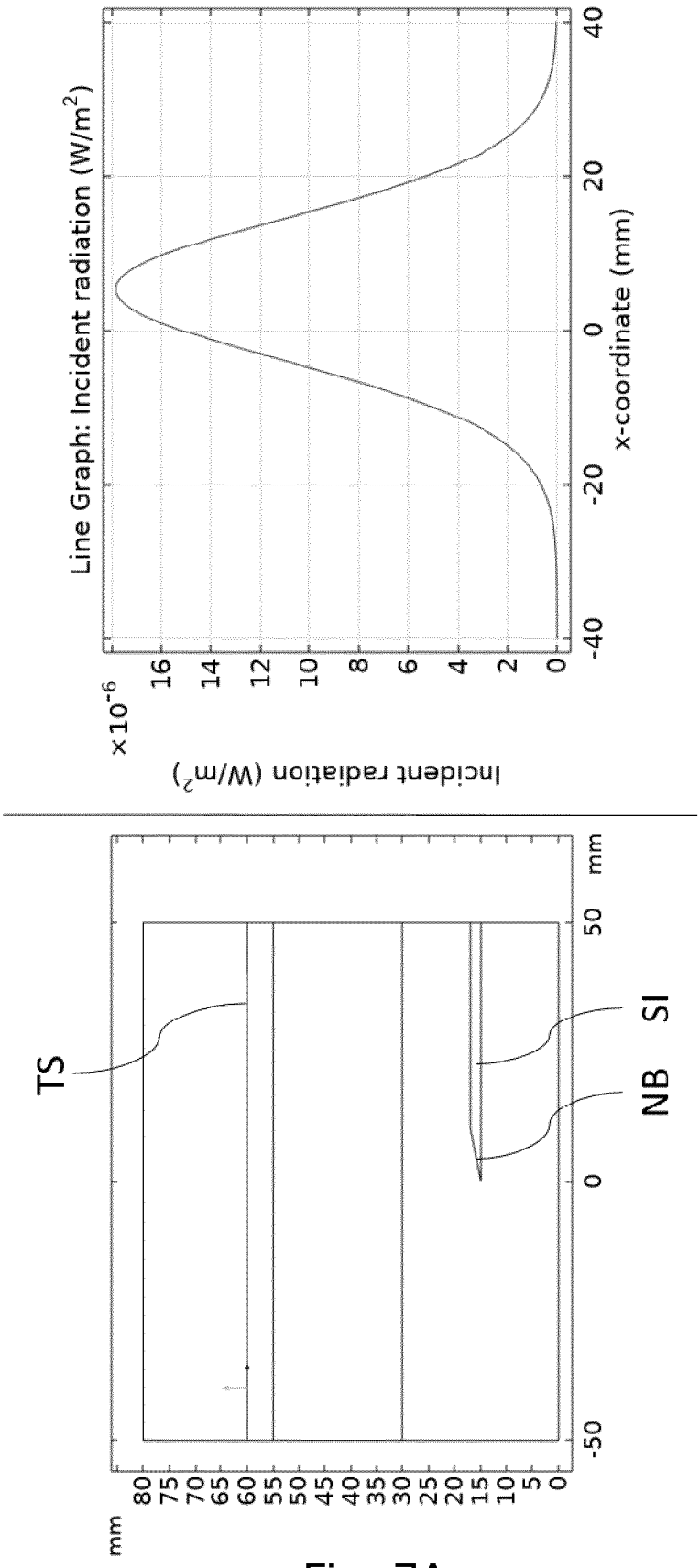
Line Graph: Incident radiation (W/m²)
x-coordinate (mm)
Incident radiation (W/m²)
×10⁻⁶
TS
SI
NB
mm
mm

Fig. 7A

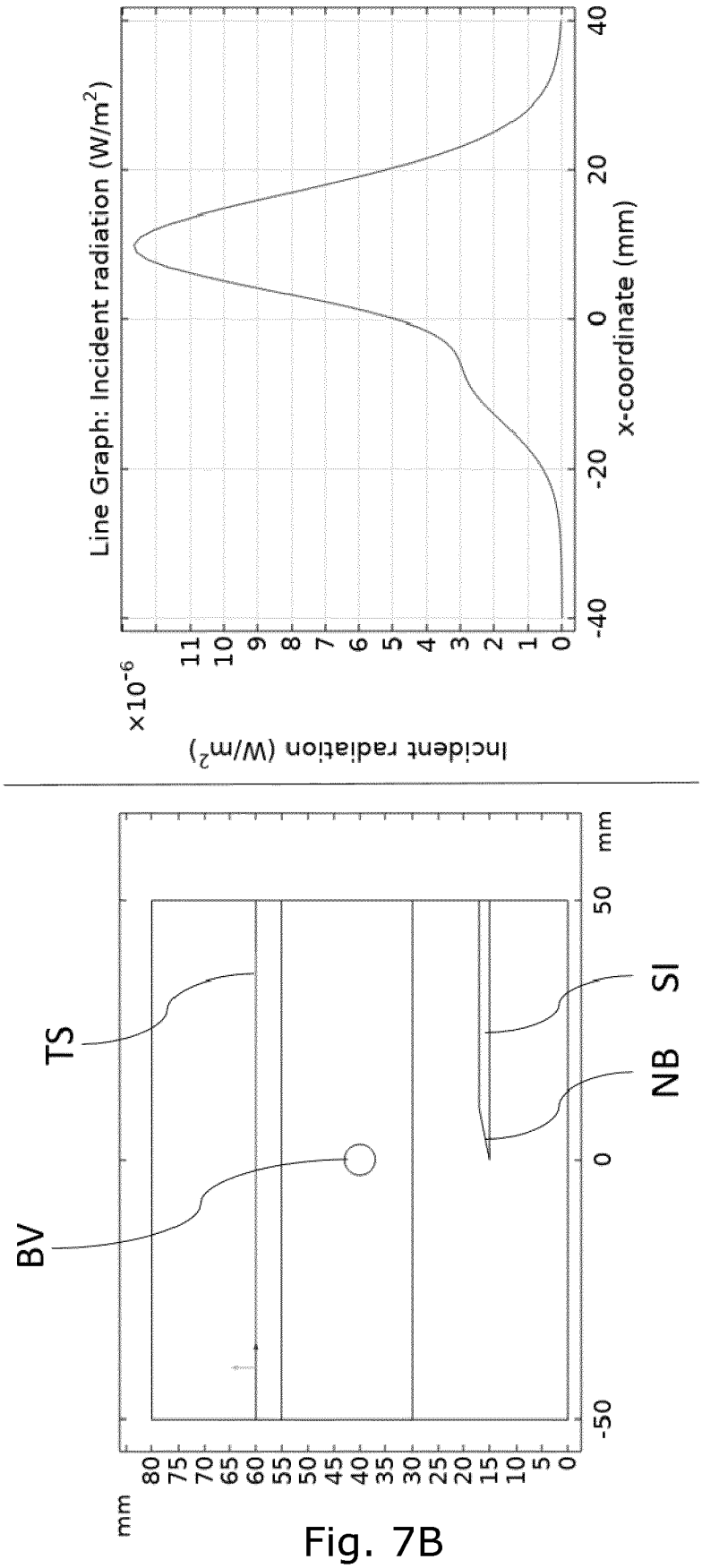
Line Graph: Incident radiation (W/m²)
x-coordinate (mm)
Incident radiation (W/m²)
×10⁻⁶
TS
BV
SI
NB
mm
mm

Fig. 7B

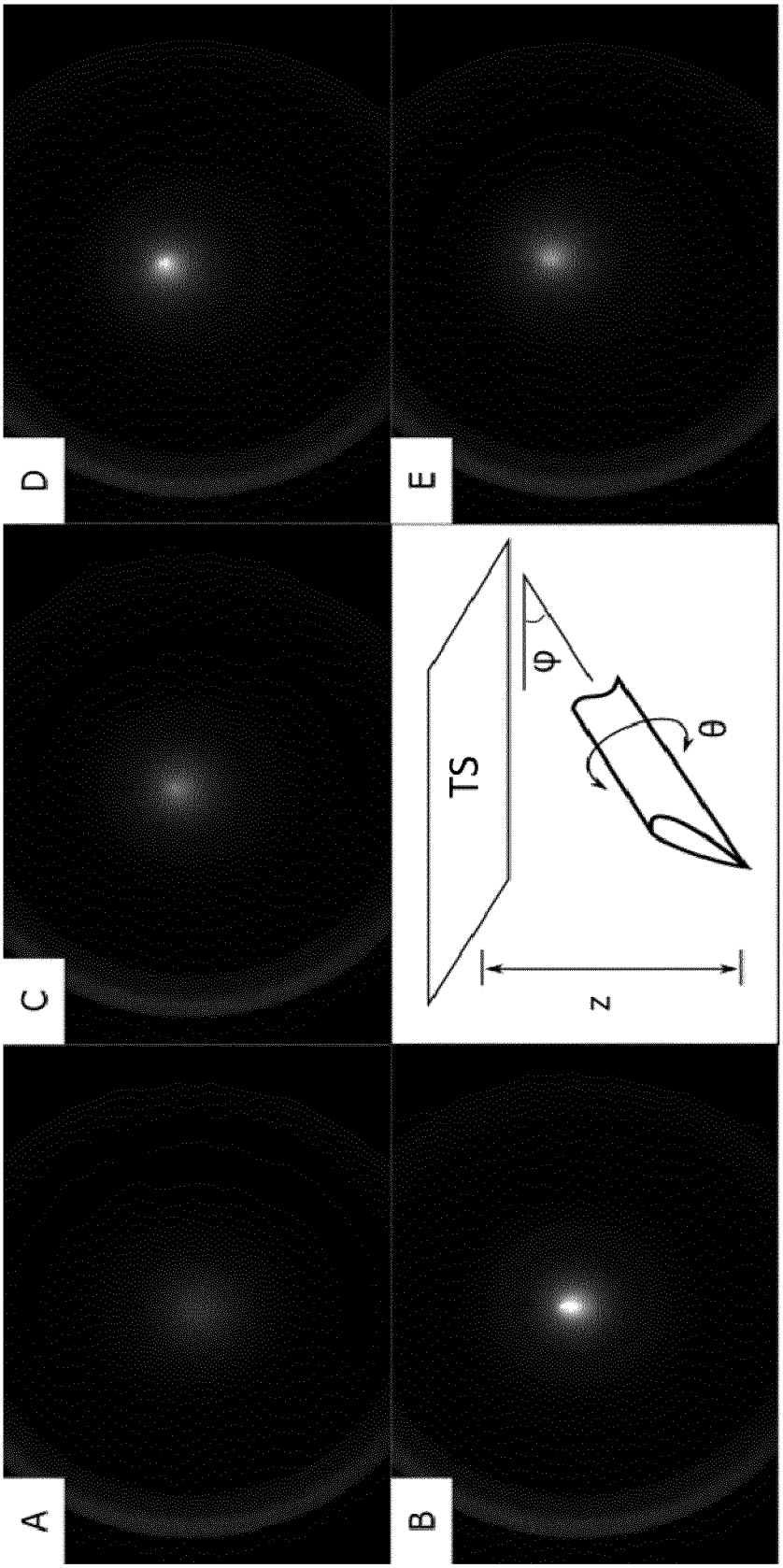

Fig. 8A - 8E

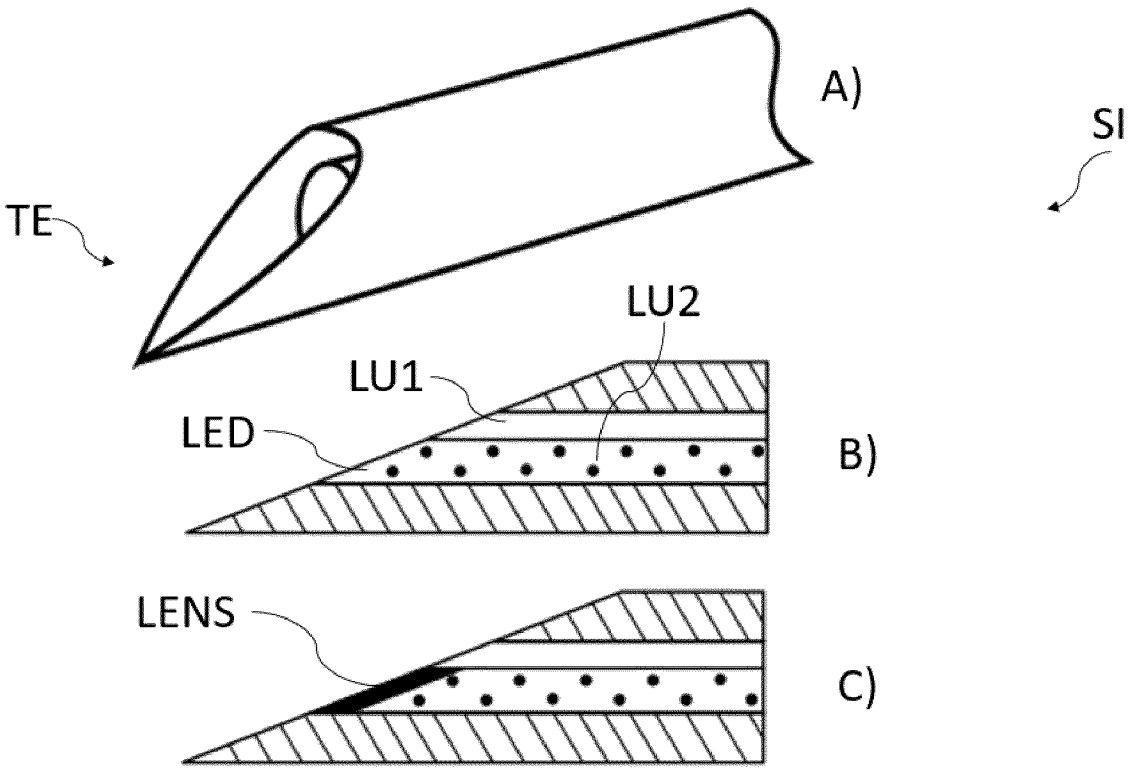

Fig. 9

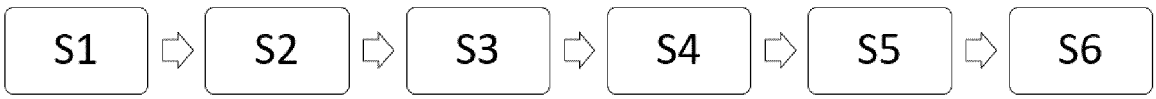

Fig. 10

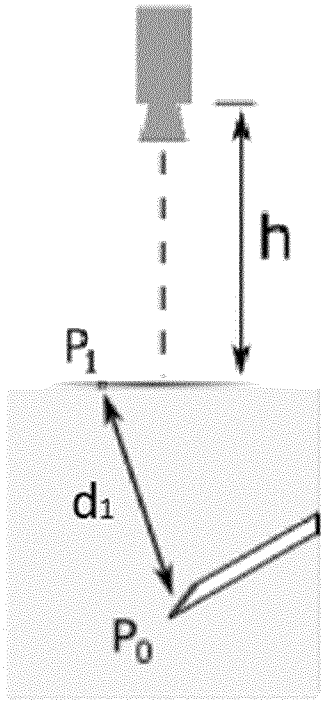

Fig. 11

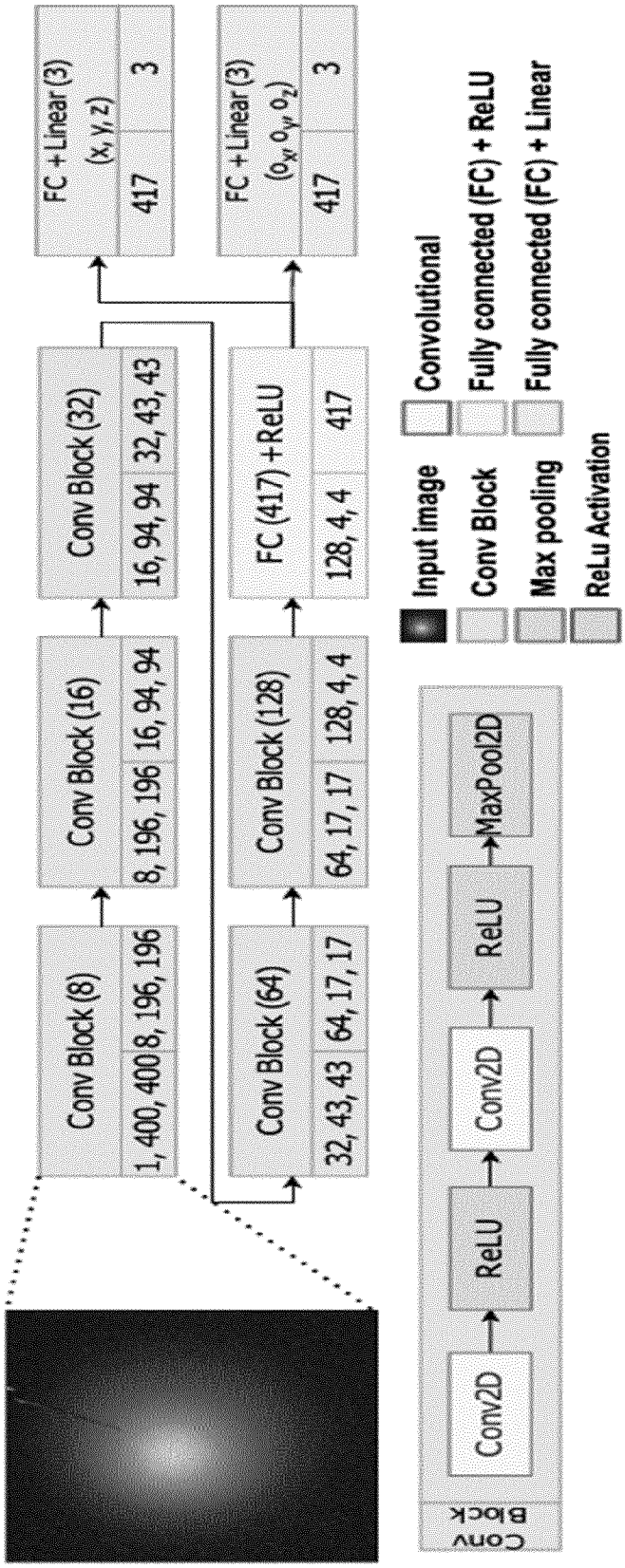
Conv Block (8)
1, 400, 400
8, 196, 196
196
Conv Block (16)
8, 196, 196
16, 94, 94
94
Conv Block (32)
16, 94, 94
32, 43, 43
43
FC + Linear (3)
(x, y, z)
417
3
Conv Block (64)
32, 43, 43
64, 17, 17
17
Conv Block (128)
64, 17, 17
128, 4, 4
4
FC (417) +ReLU
128, 4, 4
417
FC + Linear (3)
(o_x, o_y, o_z)
417
3
Input image
Convolutional
Conv Block
Fully connected (FC) + ReLU
Max pooling
Fully connected (FC) + Linear
ReLu Activation
Conv Block
Conv2D
ReLU
Conv2D
ReLU
MaxPool2D

Fig. 12

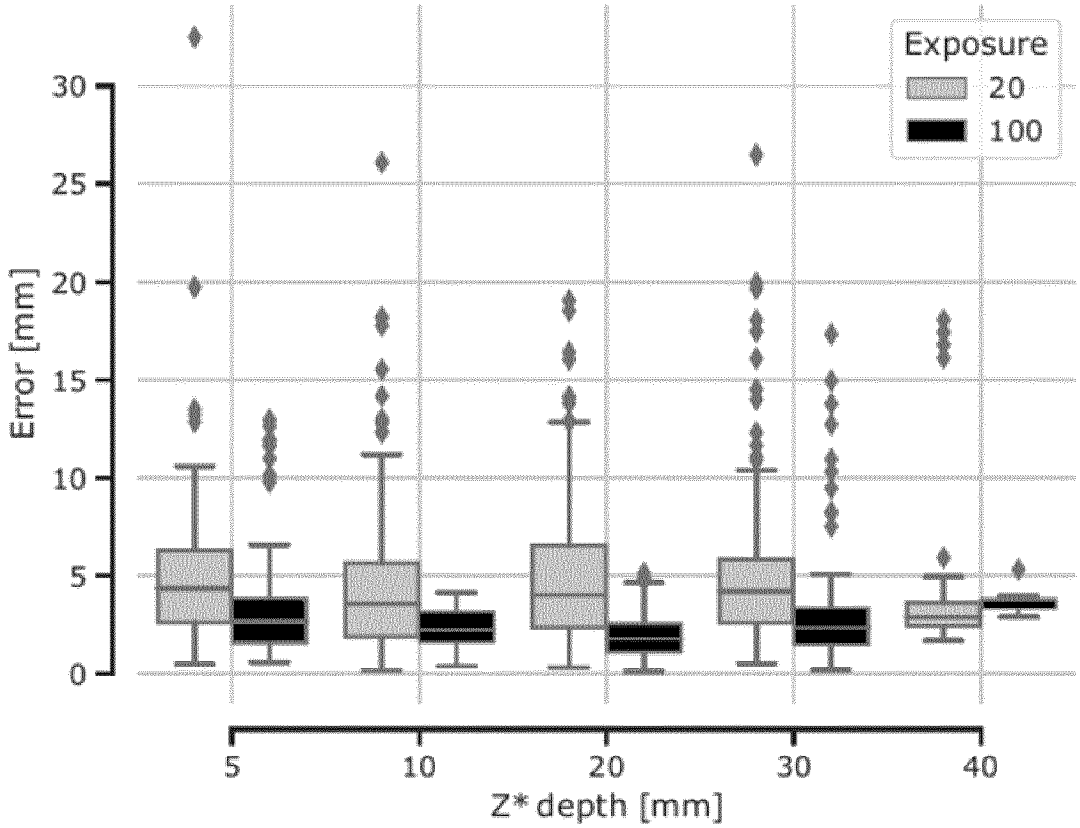

Fig. 13

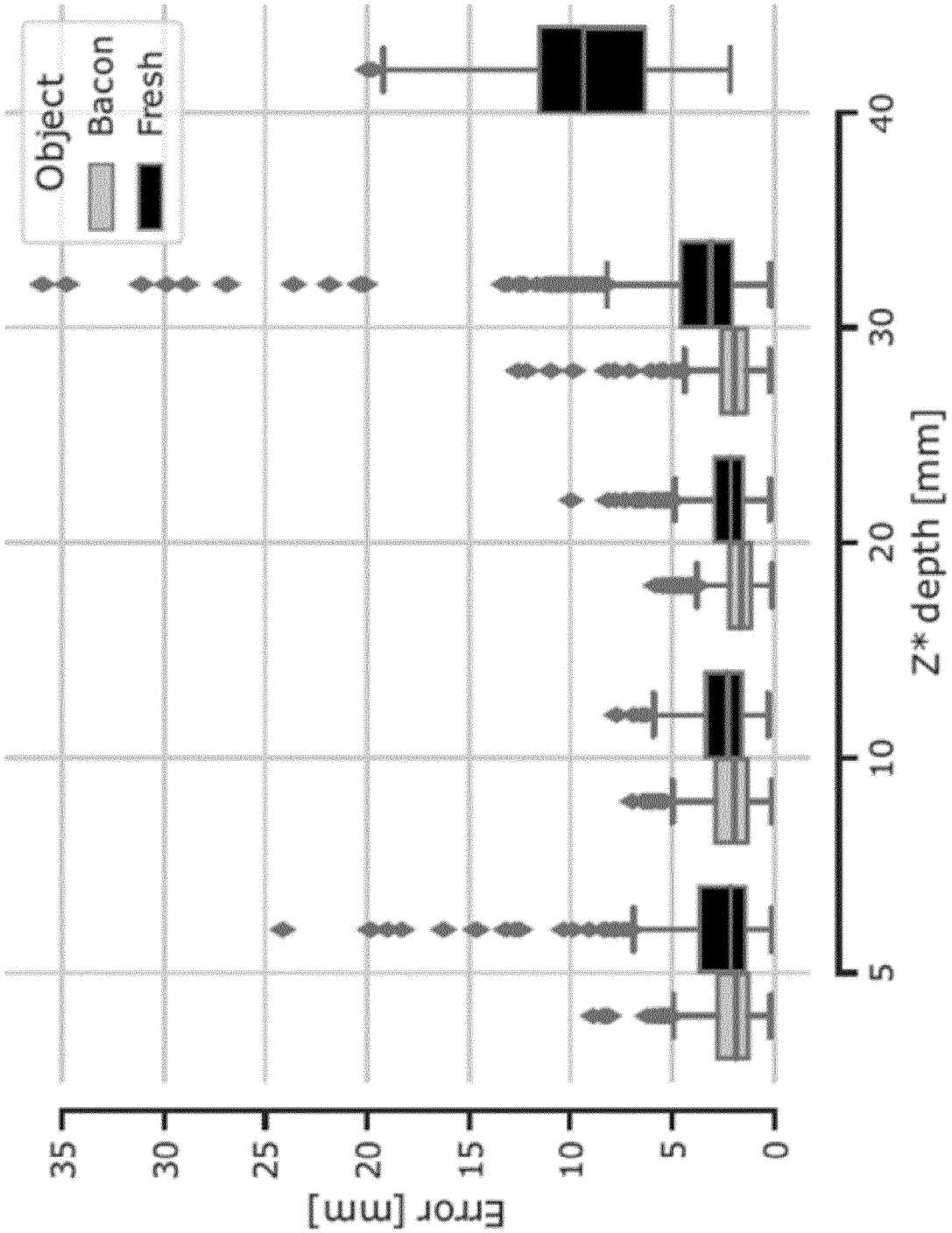
Object
Bacon
Fresh
Error [mm]
0
5
10
15
20
25
30
35
Z* depth [mm]
5
10
20
30
40

Fig. 14

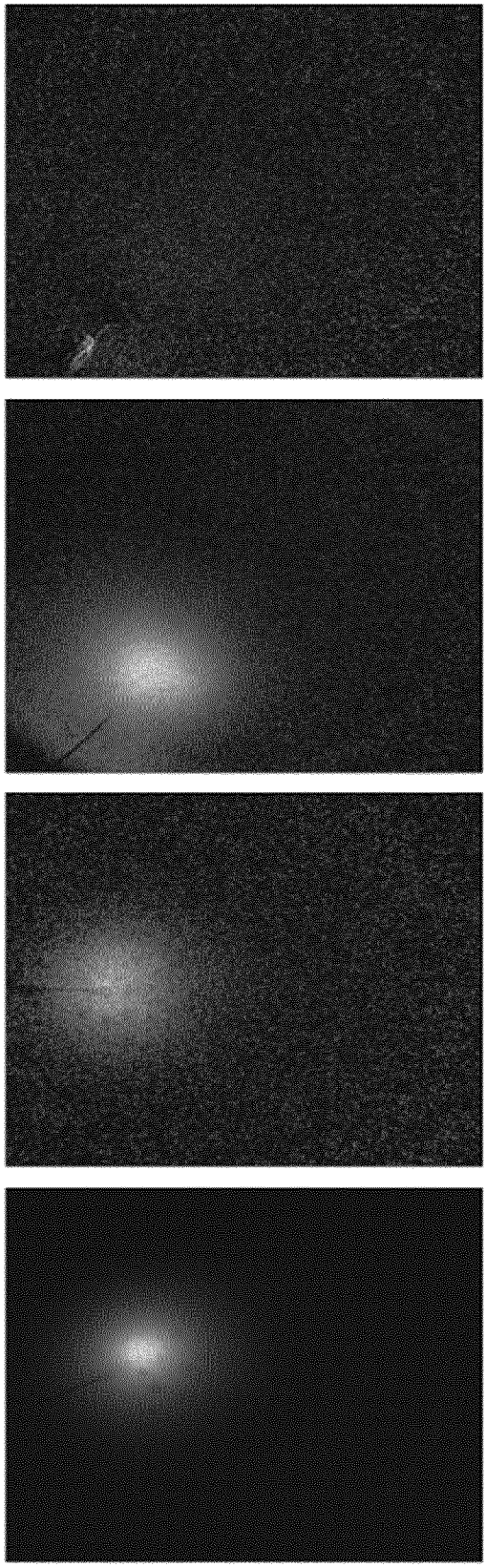

Fig. 15

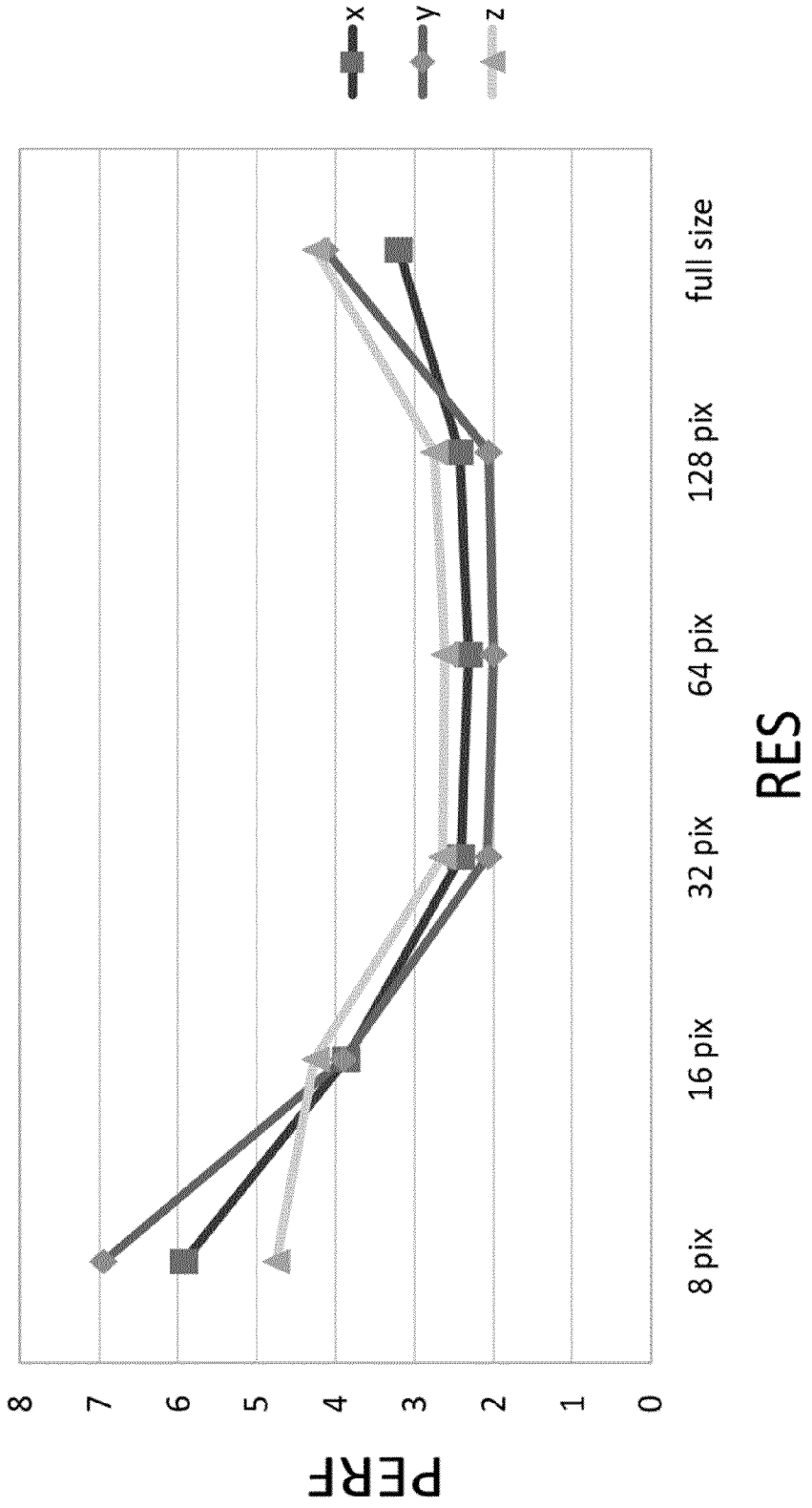
x
y
z
full size
128 pix
64 pix
32 pix
16 pix
8 pix
RES
8
7
6
5
4
3
2
1
0
PERF

Fig. 16

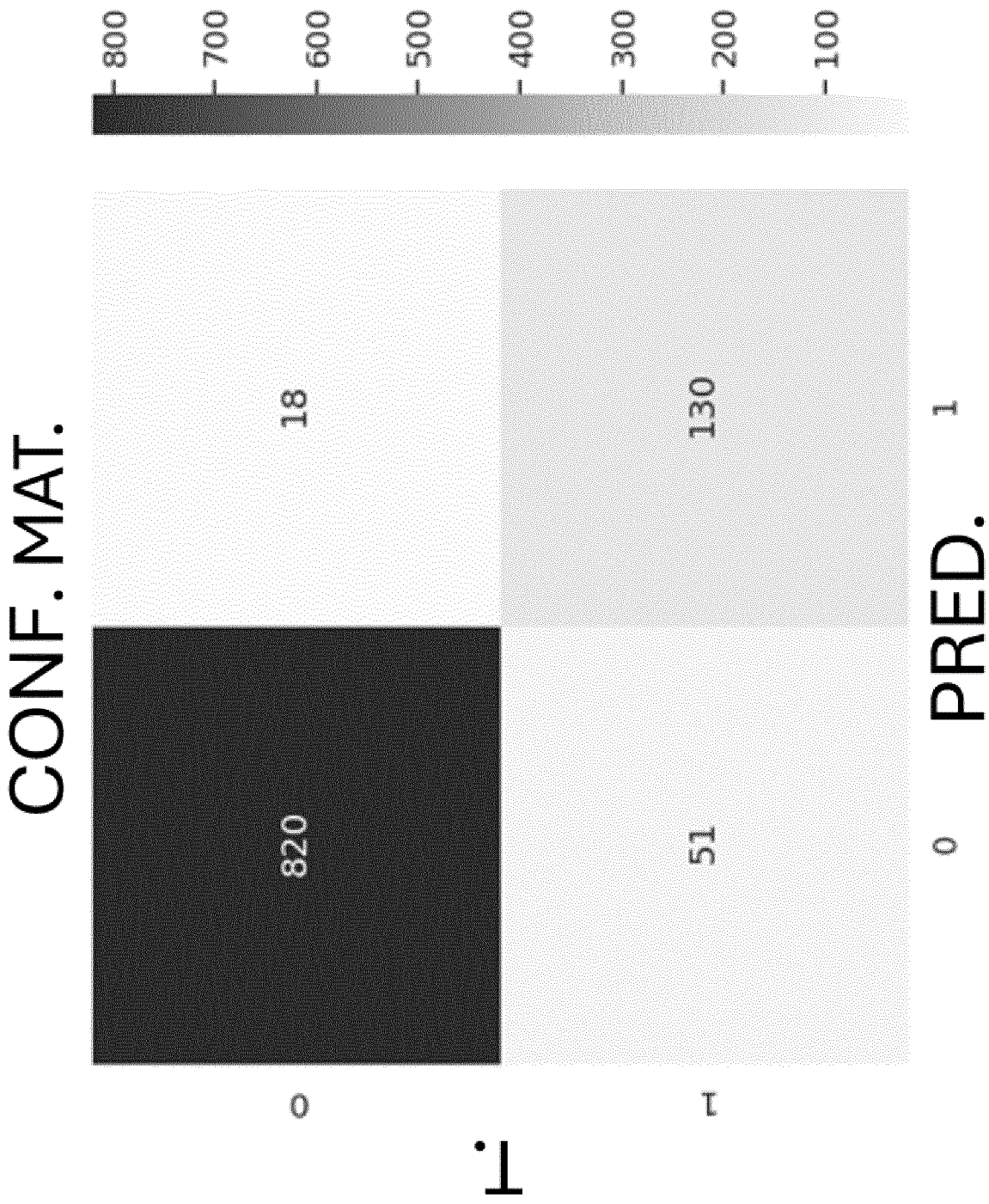
CONF. MAT.
800
700
600
500
400
300
200
100
18
130
820
51
0
1
T.
0
1
PRED.

Fig. 17

INTERNATIONAL SEARCH REPORT

International application No
PCT/EP2024/058305

A. CLASSIFICATION OF SUBJECT MATTER
INV. A61B17/34 A61B34/20 A61B5/06
ADD.

According to International Patent Classification (IPC) or to both national classification and IPC

B. FIELDS SEARCHED

Minimum documentation searched (classification system followed by classification symbols)
A61B A61M

Documentation searched other than minimum documentation to the extent that such documents are included in the fields searched

Electronic data base consulted during the international search (name of data base and, where practicable, search terms used)
EPO-Internal, WPI Data

C. DOCUMENTS CONSIDERED TO BE RELEVANT

Category*	Citation of document, with indication, where appropriate, of the relevant passages	Relevant to claim No.
X	US 2008/039715 A1 (WILSON DAVID F [US] ET AL) 14 February 2008 (2008-02-14)	13-22,33
A	figures 1, 2, 3C claim 1 claim 10 paragraph [0003] paragraph [0022] - paragraph [0023] paragraph [0026] paragraph [0089] paragraph [0116] paragraph [0120]	23-27

-/--

[x] Further documents are listed in the continuation of Box C.

[x] See patent family annex.

* Special categories of cited documents :

"A" document defining the general state of the art which is not considered to be of particular relevance

"E" earlier application or patent but published on or after the international filing date

"L" document which may throw doubts on priority claim(s) or which is cited to establish the publication date of another citation or other special reason (as specified)

"O" document referring to an oral disclosure, use, exhibition or other means

"P" document published prior to the international filing date but later than the priority date claimed

"T" later document published after the international filing date or priority date and not in conflict with the application but cited to understand the principle or theory underlying the invention

"X" document of particular relevance;; the claimed invention cannot be considered novel or cannot be considered to involve an inventive step when the document is taken alone

"Y" document of particular relevance;; the claimed invention cannot be considered to involve an inventive step when the document is combined with one or more other such documents, such combination being obvious to a person skilled in the art

"&" document member of the same patent family

Date of the actual completion of the international search	Date of mailing of the international search report
17 April 2024	30/04/2024

Name and mailing address of the ISA/	Authorized officer
European Patent Office, P.B. 5818 Patentlaan 2 NL - 2280 HV Rijswijk Tel. (+31-70) 340-2040, Fax: (+31-70) 340-3016	Cutrone, Annarita

1

Form PCT/ISA/210 (second sheet) (April 2005)

INTERNATIONAL SEARCH REPORT

International application No
PCT/EP2024/058305

C(Continuation). DOCUMENTS CONSIDERED TO BE RELEVANT

Category*	Citation of document, with indication, where appropriate, of the relevant passages	Relevant to claim No.
X	US 2020/337781 A1 (BABAZADE ROVNAT [US] ET AL) 29 October 2020 (2020-10-29)	13,
A	figures 1, 2A, 2B, 2C, 3	14-16,
	paragraph [0015]	17-20,33
	paragraph [0018]	21-27
	paragraph [0024]	
	paragraph [0026]	
	paragraph [0030] - paragraph [0031]	

X	US 2017/259013 A1 (BOYDEN EDWARD S [US] ET AL) 14 September 2017 (2017-09-14)	23,27,33
A	figures 9A, 9B	13-22,
	paragraph [0065]	24-26
	paragraph [0138]	

A	US 2007/293748 A1 (ENGVALL DANIEL [SE] ET AL) 20 December 2007 (2007-12-20)	13-27
	the whole document	

X	US 2008/097378 A1 (ZUCKERMAN STEPHEN D [US]) 24 April 2008 (2008-04-24)	23,26,33
Y	figures 1, 2, 5, 6	24,25
A	paragraph [0034] - paragraph [0036]	13-22,27
	paragraph [0057]	

Y	WO 2009/019707 A1 (IMPEDIGUIDE LTD [IL]; KENAN GAD [IL] ET AL.)	24,25
	12 February 2009 (2009-02-12)	
A	figures 14A-C	13-23,
	page 1, line 3 - line 5	26,27
	page 22, line 1 - line 3	

A	US 2014/243656 A1 (KRONSTRÖM KAI [FI] ET AL) 28 August 2014 (2014-08-28)	13-27
	the whole document	

1

INTERNATIONAL SEARCH REPORT

International application No.
PCT/EP2024/058305

Box No. II Observations where certain claims were found unsearchable (Continuation of item 2 of first sheet)

This international search report has not been established in respect of certain claims under Article 17(2)(a) for the following reasons:

1. [X] Claims Nos.: 1-12, 28-32(completely); 33(partially)
because they relate to subject matter not required to be searched by this Authority, namely:
see FURTHER INFORMATION sheet PCT/ISA/210

2. [ ] Claims Nos.:
because they relate to parts of the international application that do not comply with the prescribed requirements to such an extent that no meaningful international search can be carried out, specifically:

3. [ ] Claims Nos.:
because they are dependent claims and are not drafted in accordance with the second and third sentences of Rule 6.4(a).

Box No. III Observations where unity of invention is lacking (Continuation of item 3 of first sheet)

This International Searching Authority found multiple inventions in this international application, as follows:

1. [ ] As all required additional search fees were timely paid by the applicant, this international search report covers all searchable claims.

2. [ ] As all searchable claims could be searched without effort justifying an additional fees, this Authority did not invite payment of additional fees.

3. [ ] As only some of the required additional search fees were timely paid by the applicant, this international search report covers only those claims for which fees were paid, specifically claims Nos.:

4. [ ] No required additional search fees were timely paid by the applicant. Consequently, this international search report is restricted to the invention first mentioned in the claims;; it is covered by claims Nos.:

Remark on Protest

[ ] The additional search fees were accompanied by the applicant's protest and, where applicable, the payment of a protest fee.

[ ] The additional search fees were accompanied by the applicant's protest but the applicable protest fee was not paid within the time limit specified in the invitation.

[ ] No protest accompanied the payment of additional search fees.

FURTHER INFORMATION CONTINUED FROM PCT/ISA/ 210

Continuation of Box II.1

Claims Nos.: 1-12, 28-32(completely); 33(partially)

Claims 1-12, 28-32 and 33 (partially) relate to subject-matter considered by this Authority to be covered by the provisions of Rule 39.1(iv) PCT as it relates to a surgical method for the following reasons: (i) according to independent claim 1, the "computer implemented method" comprises the step of "determining the spatial position and orientation of a surgical instrument (..) when the surgical instrument is positioned within the tissue of a subject". Inserting a surgical instrument within a body site, that, according to the description, can be a vessel or a nasal/vaginal/rectal cavity (see p. 3, lines 1-7) involves a substantial health risk. In addition, although the claim specifies the expression "prior to the method", attempting to overcome an objection related to a surgical method, the surgical step is still limiting the scope of the claim as a method will only fall within the scope of the claim if the instrument is inserted within the tissue, being said step an essential condition. As a consequence, said surgical step is considered implicitly encompassed within the claim scope; (ii) independent claim 28 specifies a method that comprises the step of "training an algorithm" that encompasses the embodiment specified in claim 30, i.e. "the algorithm is further trained to detect the transition of position of the surgical instrument, from a first tissue to a second tissue". Said step implies the movement of the surgical instrument within the tissue which involves a substantial health risk. As a consequence, as claim 28 encompasses an embodiment addressing a surgical treatment, the method is considered to comprise a surgical step and therefore to be surgical as a whole. Therefore, claims 1-12, 28-32 and 33 (partially) have not been searched.

INTERNATIONAL SEARCH REPORT

Information on patent family members

International application No
PCT/EP2024/058305

Patent document cited in search report	Publication date	Patent family member(s)	Publication date
US 2008039715 A1	14-02-2008	AU 2008261798 A1	18-12-2008
		CA 2690572 A1	18-12-2008
		CN 101765397 A	30-06-2010
		EP 2164382 A1	24-03-2010
		JP 2010528818 A	26-08-2010
		US 2008039715 A1	14-02-2008
		WO 2008154533 A1	18-12-2008
US 2020337781 A1	29-10-2020	NONE	
US 2017259013 A1	14-09-2017	NONE	
US 2007293748 A1	20-12-2007	AT E469601 T1	15-06-2010
		AU 2005257715 A1	05-01-2006
		BR PI0512537 A	25-03-2008
		CA 2571186 A1	05-01-2006
		CN 1997312 A	11-07-2007
		DK 1768551 T3	04-10-2010
		EP 1768551 A1	04-04-2007
		ES 2348245 T3	01-12-2010
		HK 1101769 A1	26-10-2007
		IL 180323 A	31-01-2011
		JP 4831776 B2	07-12-2011
		JP 2008503318 A	07-02-2008
		KR 20070043718 A	25-04-2007
		NZ 552023 A	24-12-2009
		PL 1768551 T3	30-11-2010
		RU 2350263 C2	27-03-2009
		SG 155942 A1	29-10-2009
		SI 1768551 T1	29-10-2010
		US 2007293748 A1	20-12-2007
		WO 2006001759 A1	05-01-2006
		ZA 200610419 B	27-02-2008
US 2008097378 A1	24-04-2008	EP 1884211 A2	06-02-2008
		US 2008097378 A1	24-04-2008
		WO 2008016959 A2	07-02-2008
WO 2009019707 A1	12-02-2009	EP 2194895 A1	16-06-2010
		WO 2009019707 A1	12-02-2009
US 2014243656 A1	28-08-2014	EP 2726144 A1	07-05-2014
		US 2014243656 A1	28-08-2014
		WO 2013001510 A1	03-01-2013